

THE UNIVERSITY OF CALGARY

Nonequispaced Fourier Transform for Option Pricing

by

Li Xu

A THESIS

SUBMITTED TO THE FACULTY OF GRADUATE STUDIES  
IN PARTIAL FULFILLMENT OF THE REQUIREMENTS FOR THE  
DEGREE OF MASTER OF SCIENCE

DEPARTMENT OF MATHEMATICS AND STATISTICS

CALGARY, ALBERTA

August, 2008

© Li Xu 2008

**THE UNIVERSITY OF CALGARY**  
**FACULTY OF GRADUATE STUDIES**

The undersigned certify that they have read, and recommend to the Faculty of Graduate Studies for acceptance, a Thesis entitled “Nonequispaced Fourier Transform for Option Pricing” submitted by Li Xu in partial fulfillment of the requirements for the degree of MASTER OF SCIENCE.

---

Supervisor, Dr. A. F. Ware  
Department of Mathematics and Statistics

---

Dr. A. Swishchuk  
Department of Mathematics and Statistics

---

Dr. A. Lehar  
Haskayne School of Business

---

Date

# Abstract

This thesis investigates the applications of the nonequispaced fast Fourier transform (NFFT) in pricing various types of options under different underlying processes. We start with discrete Asian options under the exponential Lévy models and demonstrate that the NFFT algorithm offers a high order of accuracy and can be extended to approximate the continuous case. Based on the semi-Lagrangian method, we apply the NFFT to evaluate European and American options under a class of processes which includes Lévy-driven mean-reverting processes. Several numerical examples of pricing such kinds of options are presented to illustrate the efficiency of our method.

# Acknowledgements

I would like to express my gratitude to many individuals for their generous help and insightful advice during my research and study.

First and foremost, I am extremely grateful to my supervisor Dr. Tony Ware, for his invaluable guidance, inspiring advice and incredible patience. Without his continuing help, both mathematically and personally, this thesis would hardly be possible. I benefited a lot from his admirable deep knowledge in mathematical finance, and what's more, I learned how to do research from him. I must say it is my great honor to work with you.

Besides, I would like to thank my interim supervisor Dr. Anatoliy Swishchuk, for his great support and help throughout my first year of study. His courses and our research project is a memorable experience for me.

Moreover, special thanks goes to Dr. Alfred Lehar for his reading and comments, which make the thesis more satisfactory. I also wish to acknowledge Dr. Len Bos and Dr. K. C. Cheung, for their impressive courses on computational finance and stochastic processes. I should not forget my colleague Hua Li, Matt Lyle and Zhan Pang. The discussion with them is essential to my thesis and research.

Finally and most importantly, my deepest appreciation goes to my parents, for their boundless support and endless love. Thank you for giving me great confidence to succeed in my life.

# Table of Contents

Approval Page	ii
Abstract	iii
Acknowledgements	iv
Table of Contents	v
List of Figures	viii
<b>1 Introduction</b>	<b>1</b>
1.1 Financial Derivatives . . . . .	1
1.2 Modelling the Market with Lévy Processes . . . . .	4
1.2.1 Empirical Studies of the Market . . . . .	5
1.2.2 Fundamentals of Lévy Processes . . . . .	9
1.2.3 The Exponential Lévy Models . . . . .	12
<b>2 An Overview of Fourier Transform Methods</b>	<b>24</b>
2.1 Fourier Transform and Fast Fourier Transform . . . . .	24
2.2 Option Pricing with Fourier Transform . . . . .	27
2.3 Nonequispaced Fast Fourier Transform . . . . .	32
<b>3 Pricing Asian Options via the NFFT</b>	<b>36</b>
3.1 An Overview of Pricing Asian Options . . . . .	36
3.1.1 The PDE method . . . . .	38
3.1.2 The Monte Carlo method . . . . .	40
3.1.3 The FFT Method . . . . .	41
3.2 NFFT Algorithm for Asian Options . . . . .	45
3.3 Error Analysis . . . . .	48
<b>4 Numerical Examples</b>	<b>52</b>
4.1 Asian Options under the Log-normal Model . . . . .	52
4.2 Continuous Case Approximation . . . . .	58
4.3 Comparison among the Lévy Models . . . . .	61
<b>5 Option Pricing Based on the Semi-Lagrangian Method</b>	<b>65</b>
5.1 The Semi-Lagrangian Method . . . . .	65
5.2 Pricing Options through Transition Densities . . . . .	67

5.2.1	European Options under the OU Processes . . . . .	71
5.2.2	European Options under the CIR Processes . . . . .	74
5.3	Pricing Options Directly through PIDEs . . . . .	76
5.3.1	Simple Examples . . . . .	83
5.3.2	Variance Gamma-Driven OU Processes . . . . .	86
<b>6</b>	<b>Conclusion and Future Work</b>	<b>90</b>
<b>A</b>	<b>Background</b>	<b>93</b>
A.1	Statistics of Random Variables . . . . .	93
A.2	Risk-neutral Pricing Theory . . . . .	94
A.3	Gaussian Quadrature and Romberg Integration . . . . .	97
<b>B</b>	<b>Special Functions and Processes</b>	<b>99</b>
B.1	Special Functions . . . . .	99
B.2	Basic Lévy Processes . . . . .	102
	<b>Bibliography</b>	<b>104</b>

# List of Tables

1.1	Mean, standard deviation, skewness and kurtosis of major indices . . .	6
4.1	Prices of Asian options with different choice of grid width . . . . .	53
4.2	The computation time of using characteristic function and using convolution . . . . .	54
4.3	The comparison of different algorithms . . . . .	56
4.4	The comparison of the different methods for the Asian option . . . . .	59
4.5	The comparison of approximations to continuous Asian options . . . . .	60
4.6	The comparison of different methods for continuous Asian options with $S_0 = 100$ , $r = 0.09$ and $T = 1$ . . . . .	61
4.7	The comparison of Asian option prices under different Lévy models . . . . .	63
5.1	Prices of European call options under the OU process . . . . .	73
5.2	Prices of European call options under the CIR process . . . . .	76
5.3	Prices of American puts under Variance Gamma . . . . .	85
5.4	Prices of European puts under CGMY . . . . .	85
5.5	Prices of European calls under the OU process . . . . .	86
5.6	Prices of European puts under OU-VG . . . . .	88
5.7	Prices of American puts under OU-VG . . . . .	88

## List of Figures

1.1	Histogram and Q-Q plot of the daily log-returns of S&P 500 (1988-2007)	6
1.2	Historical volatility of S&P 500 (1988-2007)	8
1.3	Volatility clusters: log-returns of S&P 500 (1988-2007)	8
1.4	Variance Gamma density	17
1.5	Normal Inverse Gaussian density	20
1.6	CGMY density	21
3.1	The evolution of the probability density	44
4.1	Relative error of different algorithms	57
4.2	Densities of the log-returns in 1 year	62
4.3	Left: Density of $A_n$ under different Lévy models. Right: Density of the average under different Lévy models.	64
5.1	Left: Relative error of American puts under Variance Gamma. Right: Relative error of European puts under CGMY.	85
5.2	Relative error of European calls under the OU process.	87
5.3	Relative error of European puts (left) and American puts (right) under OU-VG.	89
5.4	Left: Comparison of European and American puts under OU-VG. Right: Comparison of American puts with different maturities under OU-VG.	89

# Chapter 1

## Introduction

### 1.1 Financial Derivatives

Financial derivatives are instruments whose values are derived from other fundamental financial assets, called the underlying assets. The main types of financial derivatives are futures, forwards, options and swaps. Such kind of derivatives have two primary uses: hedging and speculation. Market participants can hedge a risky position in an underlying asset by taking an opposing position in some financial derivatives, so that their losses can be limited to certain level regardless of any ensuring movement in the underlying asset. On the other hand, speculative investors trade derivatives to make profit according to their bets on the trends of the asset prices. In most derivatives markets, the value of speculative trading is far higher than the value of true hedge trading. Over the past several decades, derivative markets have undergone a fast development. Nowadays, the Chicago Board Options Exchange (CBOE) has an annual trade of over 450 million options contracts, covering more than 1200 companies, 50 stock indexes, and 50 exchange-traded funds (ETFs). As of approximately April 11, 2007, the Wall Street Journal estimates that globally the market capitalization of derivatives markets (futures, options, swaps, etc.) exceeds 450 trillion dollars (while US stock exchanges have approximately 30 trillion and the rest of the worlds stock exchanges total to about another 20 trillion, to a total of about 50 trillion—while global fixed income markets total to roughly

65 trillion)<sup>1</sup>.

Among the various types of financial derivatives, options are one of the most important. They give the holder the right to buy or sell some asset at a specified date at a specified price. There are several terminologies in a standard option contract. The asset on which the option is traded is known as the underlying asset. The predetermined trading date of a option is called the maturity date or the expiry date, usually denoted as  $T$ . And the price at which the trade is done at the maturity is called the strike price or the delivery price, usually denoted as  $K$ .

Options can be grouped into two styles: calls and puts. The former give the holder the right to buy an underlying asset while the latter give the right to sell the asset. Options can also be classified into several categories.

- European options. These options can only be exercised at the maturity date. Since European style options are the most basic, well studied and traded options, they are also named “vanilla options”.
- American options. These options can be exercised by the holder at any trading date before or at the maturity date.
- Bermudan options. These options allow the holder to exercise at one of a set of specified dates before or at the maturity. They are intermediate between European style options and American options.
- Asian options. The option payoff depends on the average of the underlying asset over the life of the contract.

---

<sup>1</sup>[http://en.wikipedia.org/wiki/Chicago\\_Board\\_Options\\_Exchange](http://en.wikipedia.org/wiki/Chicago_Board_Options_Exchange).

- Barrier options. The payoff for this kind of option depends on whether the underlying asset crosses the given barrier level before the maturity date.
- Spread options. The option payoff depends on the difference of two underlying assets. They are typical multi-asset options and are widely used in commodity markets.

Options with complicated payoffs or exercise styles are called “exotic options”.

The key issue in the theory of options is determining their values and hedge ratios. In 1973, Black and Scholes [12] first introduced an idea of obtaining the fair price of a European option, which paved the way for option pricing theory. They replicated the payoff of a option by constructing a portfolio containing the underlying and a bond. This idea leads to a partial differential equation (PDE) and an analytical pricing formula for the option (see [73]). When such analytical forms of option prices are not available, various numerical methods have been developed to price options, for example, tree methods [24], Monte Carlo simulation [14], finite difference method [73], Fourier transform [17], etc. One essential technique that should be introduced in this thesis, is named risk-neutral pricing approach (see [37]). In short, if there exists a risk-neutral measure  $\mathbb{Q}$  (a probability measure in which there is no arbitrage in the market), the price of any options can be represented by the expectation of the discounted payoff under the risk-neutral measure:

$$V(S, T) = \mathbb{E}^{\mathbb{Q}}[e^{-rT}(f(S, K, T))] \quad (1.1)$$

where  $S$  is the spot price of the underlying,  $K$  is the strike price,  $T$  is the maturity date and  $r$  is the risk free rate.  $f(S, K, T)$  and  $V(S, T)$  stand for the payoff function

and the value of the option, respectively. Details about the risk-neutral pricing theory are given in [37, 63], and some background is briefly introduced in Appendix A.2.

Options with any kind of payoff can be evaluated in this setting. Though the risk-neutral measure is not unique when the market is incomplete, there are several ways to find such a risk-neutral measure (see [35] for example). In this thesis, we do not focus on this topic and always assume that we are in the risk-neutral world.

## 1.2 Modelling the Market with Lévy Processes

In order to obtain accurate prices for financial derivatives, the first stage is to model the underlying market correctly; that is, we must find some suitable processes which are able to capture the essential behaviour of the underlying prices. The most famous model is the log-normal model [12] in which the log-return of the asset price is assumed to be normally-distributed. However, numerous empirical studies of market data show that this is not the case (see [21]). Hence, more flexible distributions and processes should be introduced to describe the stochastic dynamics of the asset returns. For example, in energy and interest rate markets, mean-reverting processes like the Ornstein-Uhlenbeck (OU) process or the Cox-Ingersoll-Ross (CIR) process are widely used. Lévy processes, a class of processes with independent and stationary increments, which are named after Paul Lévy, were also introduced to model the financial market. In this section, we are going to give a brief introduction to Lévy processes. In Section 1.2.1, the empirical properties of the asset returns and the motivation for using Lévy processes are discussed. The definition and important

properties of Lévy processes are introduced in Section 1.2.2. Examples of several popular Lévy processes and market models under these processes are described in Section 1.2.3.

### 1.2.1 Empirical Studies of the Market

In the log-normal model, the stochastic dynamics of the asset prices are described by the stochastic differential equation (SDE):

$$dS_t = \mu S_t dt + \sigma S_t dW_t, \quad (1.2)$$

where  $S_t$  is the asset price at time  $t$ ,  $\mu$  and  $\sigma$  are called the drift and the volatility respectively, and  $W_t$  denotes the Brownian motion. Itô's formula gives us the solution to (1.2) as:

$$S_t = S_0 e^{(\mu - \frac{\sigma^2}{2})t + \sigma W_t}. \quad (1.3)$$

We find that there are two basic assumptions in this model. One is the normal distribution of the log-returns, since the stochastic noise is modelled by a Brownian motion. The other is the constant volatility. However, empirical evidence contradicts these two aspects.

#### Non-normal distribution

To study the statistics of the empirical distribution, we focus on the standard moments (see Appendix A.1) of the market data.

In Table 1.1, we summarize the empirical standard moments of the log-returns for a set of popular indices (quoted from [62]). The empirical distributions typically show negative skewness and high leptokurticity, so that the distribution has higher

Table 1.1: Mean, standard deviation, skewness and kurtosis of major indices

Index	Mean	Std.	Skewness	Kurtosis
S&P 500 (1988-2007)	0.0003	0.0099	-0.2416	7.32
S&P 500 (1997-1999)	0.0009	0.0119	-0.4409	6.94
Nasdaq-Composite	0.0015	0.0154	-0.5439	5.78
DAX	0.0012	0.0157	-0.4314	4.65
SMI	0.0009	0.0141	-0.3584	5.35
CAC-40	0.0013	0.0143	-0.2116	4.63

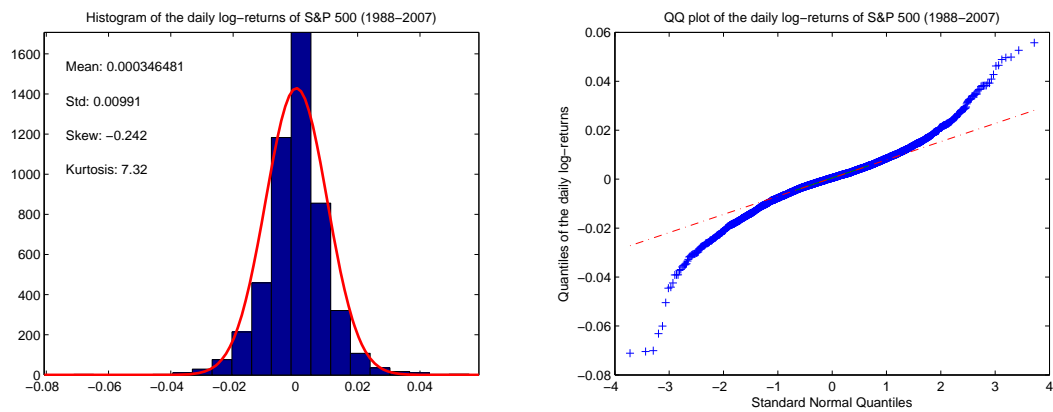


Figure 1.1: Histogram and Q-Q plot of the daily log-returns of S&amp;P 500 (1988-2007)

peak or fatter tails than the normal distribution. As an illustration, the left hand side of Figure 1.1 shows a histogram of the daily log-returns of S&P 500 (1988-2007) with a fit of a normal distribution superimposed. We find that the empirical distribution is leptokurtic. On the right hand side of Figure 1.1, we show the same comparison using a Q-Q plot. Obviously, the plot is not linear which implies the non-normal distribution of the empirical data.

## Stochastic Volatility

From empirical data, another important phenomenon is that the volatility of the log-return series also has stochastic or at least time-varying behaviour over time. This can be seen from the phenomena called historical volatility and volatility clusters.

The *historical volatility* is the realized standard deviation of the daily log-returns estimated from the historical (weekly, monthly, quarterly, yearly) data preceding that trading day. In Figure 1.2, the historical volatility for the S&P 500 (1988-2007) is obviously not a constant. The *volatility clusters* means that there seems to be a succession of periods with high return variance and with low return variance. In Figure 1.3, we observe that large price variations are more likely to be followed by large price variations. Due to such empirical evidence, lots of stochastic volatility models have been proposed and studied.

From the discussion above, the log-normal assumption is not reasonable to explain the empirical behaviour of the log-return series in skewness and kurtosis. We need a generalized version of the Brownian motion to capture these properties. Lévy processes are such processes which have more general infinitely divisible distributions than the normal one and are able to represent the negative skewness and high leptokurticity of the empirical distributions. Popular models of this type are for example, the Variance Gamma [50, 51], the Normal Inverse Gaussian [7, 8], the CGMY [16], the (Generalized) Hyperbolic Model [28] and the Meixner distributions [61]. In terms of stochastic volatility, sophisticated models based on popular Lévy processes have also been developed in [15].

The definition of Lévy processes and details about some popular models will be introduced in the following two sections.

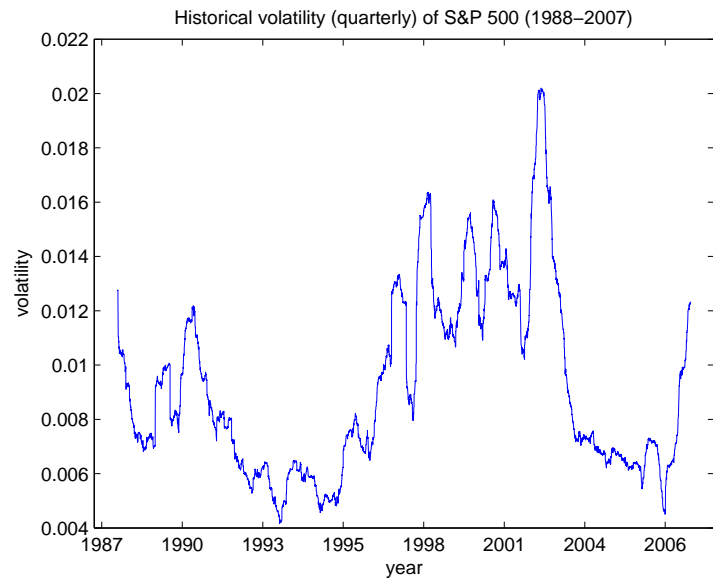


Figure 1.2: Historical volatility of S&P 500 (1988-2007)

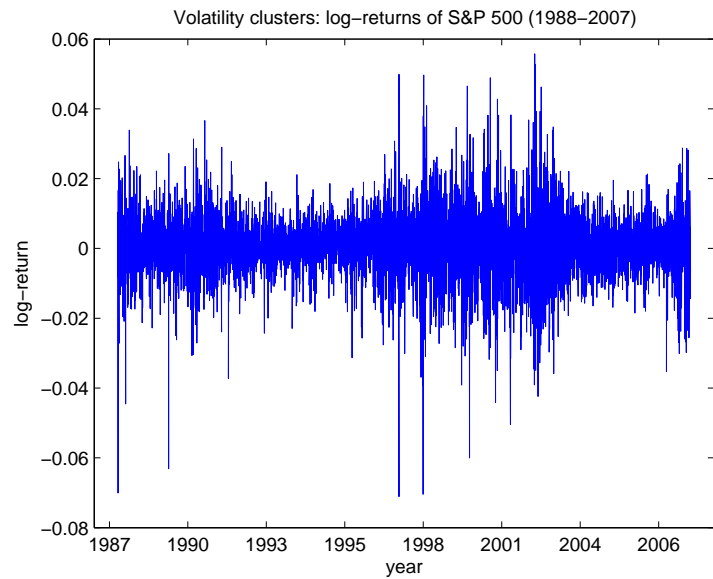


Figure 1.3: Volatility clusters: log-returns of S&P 500 (1988-2007)

### 1.2.2 Fundamentals of Lévy Processes

In this section, we present a brief introduction to Lévy processes. Other reference on Lévy processes can be found in Applebaum [6], Cont [22] and Sato [43].

**Definition 1.2.1** (Lévy Process). A càdlàg, real valued stochastic process  $(X_t)_{t \geq 0}$  on a filtered probability space  $(\Omega, \mathcal{F}, \mathbb{P})$  with  $X_0 = 0$  is called a Lévy process if it satisfies the following conditions:

1. Independent increments: for any  $0 \leq s < t \leq T$ , the increment  $X_t - X_s$  is independent of  $\mathcal{F}_s$ .
2. Stationary increments: for any  $s, t \geq 0$ , the distribution of  $X_{t+s} - X_t$  does not depend on  $t$ .
3. Stochastic continuity: for any  $t \geq 0$  and  $\varepsilon > 0$ ,  $\lim_{s \rightarrow t} \mathbb{P}(|X_t - X_s| > \varepsilon) = 0$ .

There is a celebrated proposition for a given Lévy process, called Lévy-Itô decomposition.

**Proposition 1.2.2** (Lévy-Itô decomposition). *Let  $(X_t)_{t \geq 0}$  be a Lévy process, then there exists a triplet  $(\gamma, \sigma^2, \nu)$ , with  $\gamma \in \mathbb{R}$ ,  $\sigma^2 \geq 0$  and  $\nu$  a measure on  $\mathbb{R} \setminus \{0\}$  satisfying  $\int_{\mathbb{R}} (1 \wedge |x|^2) \nu(dx) < \infty$ , such that*

$$X_t = \gamma t + \sigma W_t + X_t^l + \lim_{\epsilon \rightarrow 0} \tilde{X}_t^\epsilon, \quad (1.4)$$

where

$$X_t^l = \int_0^t \int_{|x| \geq 1} x J_X(ds \times dx),$$

and

$$\begin{aligned}\tilde{X}_t^\epsilon &= \int_0^t \int_{\epsilon \leq |x| < 1} x \tilde{J}_X(ds \times dx) \\ &= \int_0^t \int_{\epsilon \leq |x| < 1} x [J_X(ds \times dx) - \nu(dx)ds].\end{aligned}$$

$J_X$  is denoted as the Poisson random measure with intensity  $\nu(dx)dt$  and  $\tilde{J}_X$  is the compensated version of  $J_X$ .

The proposition tells us that every Lévy process is characterized by the *Lévy triplet*  $(\gamma, \sigma^2, \nu)$ . And  $\gamma$  denotes the drift term,  $\sigma^2$  is the diffusion coefficient and  $\nu$  stands for the pure jump part which is also called the *Lévy measure*.

Another important concept for a Lévy process is the characteristic function, which plays a vital role for a real-valued random variable in probability theory.

**Definition 1.2.3** (Characteristic function). The characteristic function of a real valued random variable  $X$  is defined by:

$$\phi_X(u) = \mathbb{E}[\exp(iuX)] = \int_{\mathbb{R}} e^{iux} dF_X(x). \quad (1.5)$$

Actually, it is the Fourier transform of the distribution function  $F_X(x)$  of this random variable. The characteristic function of a random variable completely characterizes its law: two variables with the same characteristic function are identically distributed. A characteristic function is always continuous and verifies  $\phi_X(0) = 1$ . And its logarithm is called the *characteristic exponent* denoted by  $\psi(u)$ .

There is strong interplay between Lévy processes and infinitely divisible distributions.

**Definition 1.2.4** (Infinite divisibility). The distribution of a random variable  $X$  is infinitely divisible if, for all  $n \in \mathbb{N}$ , there exists a random variable  $X^{(1/n)}$  such that

$$\phi_X(u) = (\phi_{X^{(1/n)}}(u))^n. \quad (1.6)$$

**Theorem 1.2.5** (Lévy-Khintchine formula). *A random variable  $X$  has infinitely divisible distribution if and only if there exists a triplet  $(\gamma, \sigma^2, \nu)$ , with  $\gamma \in \mathbb{R}$ ,  $\sigma^2 \geq 0$  and  $\nu$  a measure on  $\mathbb{R} \setminus \{0\}$  satisfying  $\int_{\mathbb{R}} (1 \wedge |x|^2) \nu(dx) < \infty$ , such that*

$$\psi(u) = i\gamma u - \frac{\sigma^2 u^2}{2} + \int_{\mathbb{R}} (e^{iux} - 1 - iux 1_{\{|x|<1\}}) \nu(dx). \quad (1.7)$$

**Proposition 1.2.6** (Infinite divisibility and Lévy processes). *Let  $(X_t)_{t \geq 0}$  be a Lévy process. Then for every  $t$ ,  $X_t$  has an infinitely divisible distribution. Conversely, if  $F$  is an infinitely divisible distribution, then there exists a Lévy process  $X_t$  such that the distribution of  $X_1$  is given by  $F$ .*

For a Lévy process corresponding to its infinitely divisible distribution, the triplet  $(\gamma, \sigma^2, \nu)$  in the Lévy-Khintchine formula is just the Lévy triplet of this process.

**Definition 1.2.7** (Infinitesimal generator). The infinitesimal generator  $\mathcal{L}$  of a Lévy process with triplet  $(\gamma, \sigma^2, \nu)$  acts on a twice-differentiable function  $f(x)$  as follows:

$$\mathcal{L}f(x) = \gamma \frac{\partial f}{\partial x} + \frac{\sigma^2}{2} \frac{\partial^2 f}{\partial x^2} + \int [f(x+y) - f(x) - y 1_{|y|<1} \frac{\partial f}{\partial x}(x)] \nu(dy). \quad (1.8)$$

By the differentiation property of the Fourier transform (see Chapter 2 below):

$$\mathcal{F}(f^{(n)}(x)) = (i\omega)^n \mathcal{F}(f(x)),$$

we have a nice expression for this infinitesimal generator  $\mathcal{L}$  on a function  $f$  after

taking the Fourier transform:

$$\begin{aligned}\mathcal{F}[\mathcal{L}f](\omega) &= \left\{i\gamma\omega - \frac{\sigma^2\omega^2}{2} + \int_{\mathbb{R}} (e^{i\omega y} - 1 - i\omega y 1_{\{|y|<1\}})\nu(dy)\right\} \cdot \mathcal{F}[f](\omega) \\ &= \psi(\omega) \cdot \mathcal{F}[f](\omega),\end{aligned}\tag{1.9}$$

where  $\psi(\omega)$  is the characteristic exponent by Lévy-Khintchine formula.

From the discussion above, given a infinitely divisible distribution, we can construct an associated Lévy process which is uniquely characterized by its characteristic function according to the Lévy-Khintchine formula. As long as the explicit form of the characteristic function is available, we can take advantage of the Fourier transform to evaluate the density function by taking the inverse Fourier transform of its characteristic function. Besides, with the Fourier transform, the complicated infinitesimal generator on a function can be simplified to its explicit characteristic exponent times the Fourier transform of this function. Therefore, Fourier transform method is very flexible to deal with option pricing problems regardless the distribution of the underlying returns. In the next section, we will give some examples of the popular Lévy processes with the closed forms of their characteristic functions.

### 1.2.3 The Exponential Lévy Models

Instead of using the Brownian motion with drift in (1.3), we could replace it with a Lévy process. Then the asset price would be modelled as:

$$S_t = S_0 e^{X_t},\tag{1.10}$$

where  $(X_t)_{t \geq 0}$  is a Lévy process. This market model is an exponential Lévy model. The log-returns,  $\log(S_{t+\Delta t}/S_t)$ , of such a model have independent and stationary increments, which are distributed according to an infinitely divisible distribution.

As outlined in Appendix A.2, the fact that the price process is driven by a Lévy process makes the market, in general, incomplete; the only exceptions are the markets driven by the log-normal (Black-Scholes model) and Poisson distributions. The incompleteness of the market means there exists many equivalent martingale measure (EMM) we could choose. One way to choose such a measure is to require the measure to be mean correcting. We denote by  $m$  the mean of the infinitely divisible distribution corresponding to the Lévy process  $X_t$ . We need to choose an appropriate measure  $\mathbb{Q}$  such that the new mean  $\tilde{m}$  of the new Lévy process  $\tilde{X}_t$  makes the discounted asset price a martingale. Let  $\tilde{m} = m + r + \omega$ , then the asset price is modelled as:

$$S_t = S_0 e^{\tilde{X}_t} = S_0 e^{rt + \omega t + X_t}, \quad (1.11)$$

where  $\omega$  is determined by setting  $\exp(-\omega t) = \phi_X(-i, t)$  or equivalently  $\mathbb{E}^{\mathbb{Q}}[e^{X_t}] = \exp(-\omega t)$ , and  $\tilde{X}_t$  is a Lévy process under this new probability measure. If such  $\omega$  is chosen, the discounted asset price  $\exp(-rt)S_t = S_0 \exp(\omega t + X_t)$  is definitely a martingale. The construction of martingale under Lévy processes is also briefly introduced in Appendix A.2.

Throughout, we assume an appropriate risk-neutral martingale measure  $\mathbb{Q}$  has been chosen in this way. Then, under such a risk-neutral measure  $\mathbb{Q}$ , the asset price is modelled as an exponential Lévy process as (1.11); the discounted asset price is a martingale and the risk-neutral pricing formula will apply.

### Log-normal Model

The famous log-normal model is just a special case of the exponential Lévy model. If we let  $X_{\text{LN}}(t) = \sigma W_t$ , we can find the risk-neutral measure by mean correcting as

mentioned in the last section. In this case, we have  $\omega = -\sigma^2/2$  so that the asset price follows:

$$S_t = S_0 e^{(r-\sigma^2/2)t + \sigma W_t}, \quad (1.12)$$

which is exactly the same as the one in the classic log-normal model.

Under the mean-corrected risk-neutral measure, the density function of  $X_{\text{LN}}(t)$  is:

$$f_{\text{LN}}(x) = \frac{1}{\sigma\sqrt{2\pi t}} \exp\left(-\frac{x^2}{2\sigma^2 t}\right). \quad (1.13)$$

The Lévy triplet is  $(0, \sigma^2, 0)$ , and the characteristic function is given by:

$$\phi_{\text{LN}}(u, t) = \exp\left(-\frac{\sigma^2 u^2}{2} t\right). \quad (1.14)$$

The standard moments of  $X_{\text{LN}}(t)$  are as follows:

Standard moments of $X_{\text{LN}}(t)$	
Mean	0
Variance	$\sigma^2 t$
Skewness	0
Kurtosis	3

We can see that  $\sigma$  is the shape parameter.

### Merton's Jump Diffusion Model

The Merton's jump diffusion process  $X_{\text{MJD}}(t)$  can be defined as a Brownian motion plus a compound Poisson process:

$$X_{\text{MJD}}(t) = \sigma W_t + \sum_{i=1}^{N_t} Y_i, \quad (1.15)$$

where  $\sigma$  is the volatility of the Brownian motion  $W_t$ ,  $N_t$  is a Poisson process with intensity  $\lambda$  and  $Y_i$  denotes the  $i$ th jump size. In the Merton's model,  $Y_i$  is normally i.i.d with mean  $\alpha$  and variance  $\delta^2$ . The density of  $Y_i$  is given by:

$$f_Y(y) = \frac{1}{\delta\sqrt{2\pi}} \exp\left(-\frac{(y-\alpha)^2}{2\delta^2}\right). \quad (1.16)$$

So the Merton's jump diffusion process is a four parameter process  $X_{\text{MJD}}(t; \sigma, \lambda, \alpha, \delta)$ .

The Lévy triplet is  $(0, \sigma^2, \lambda f_Y)$ , and the characteristic function is given by:

$$\phi_{\text{MJD}}(u, t) = \exp\left[-\frac{\sigma^2 u^2}{2}t + \lambda t(e^{iu\alpha - \delta^2 u^2/2} - 1)\right]. \quad (1.17)$$

The standard moments of  $X_{\text{MJD}}(t)$  are as follows:

Standard moments of $X_{\text{MJD}}(t)$	
Mean	$\lambda\alpha t$
Variance	$(\sigma^2 + \lambda\delta^2 + \lambda\alpha^2)t$
Skewness	$\frac{\lambda\alpha(\alpha^2 + 3\delta^2)}{(\sigma^2 + \lambda\delta^2 + \lambda\alpha^2)^{3/2}t^{1/2}}$
Kurtosis	$3 + \frac{\lambda(\alpha^4 + 3\delta^4 + 6\alpha^2\delta^2)}{(\sigma^2 + \lambda\delta^2 + \lambda\alpha^2)^2 t}$

We can see that  $\alpha$  is a skewness parameter. Larger values for  $\lambda$  and  $\sigma$  lead to larger variance and smaller kurtosis.

Under the mean-corrected risk neutral measure, the asset price is given by:

$$S_t = S_0 \exp(rt + \omega t + X_{\text{MJD}}(t; \sigma, \lambda, \mu, \delta)), \quad (1.18)$$

where

$$\omega = -\frac{\sigma^2}{2} + \lambda \left(1 - \exp\left(\alpha + \frac{\delta^2}{2}\right)\right).$$

### Variance Gamma Model

The Variance Gamma (VG) process  $X_{\text{VG}}(t; \sigma, \nu, \theta)$  is defined by time-changed Brownian motion with drift:

$$X_{\text{VG}}(t; \sigma, \nu, \theta) = W(\gamma(t; 1, \nu); \theta, \sigma).$$

The time  $t$  in the Brownian is changed to a gamma process (see Appendix B.2) with unit mean rate:  $\gamma(t; 1, \nu)$ . The VG process has three parameters: (i)  $\sigma$  the volatility of the Brownian motion, (ii)  $\nu$  the variance rate of the gamma time change and (iii)  $\theta$  the drift in the Brownian motion.

The density function of  $X_{\text{VG}}(t)$  is given by:

$$\begin{aligned} f_{\text{VG}}(x) &= \int_0^\infty \frac{1}{\sigma\sqrt{2\pi}g} \exp\left(-\frac{(x-\theta g)^2}{2\sigma^2 g}\right) \frac{g^{\frac{t}{\nu}-1} \exp\left(-\frac{g}{\nu}\right)}{\nu^{\frac{t}{\nu}} \Gamma\left(\frac{t}{\nu}\right)} dg \\ &= \frac{2 \exp(\theta x/\sigma^2)}{\nu^{t/\nu} \sqrt{2\pi} \sigma \Gamma\left(\frac{t}{\nu}\right)} \left(\frac{x^2}{2\sigma^2/\nu + \theta^2}\right)^{\frac{t}{2\nu}-\frac{1}{4}} K_{\frac{t}{\nu}-\frac{1}{2}}\left(\frac{1}{\sigma^2} \sqrt{x^2(2\sigma^2/\nu + \theta^2)}\right). \end{aligned} \quad (1.19)$$

where  $K$  is the modified Bessel function of the second kind (see Appendix B.1). The characteristic function is given by:

$$\phi_{\text{VG}}(u, t) = \left(\frac{1}{1 - i\theta\nu u + (\sigma^2\nu/2)u^2}\right)^{t/\nu}, \quad (1.20)$$

with Lévy measure:

$$k_{\text{VG}}(x) = \frac{\exp(\theta x/\sigma^2)}{\nu|x|} \exp\left(-\frac{\sqrt{2\sigma^2/\nu + \theta^2}}{\sigma^2}|x|\right). \quad (1.21)$$

The standard moments of  $X_{\text{VG}}(t)$  are as follows:

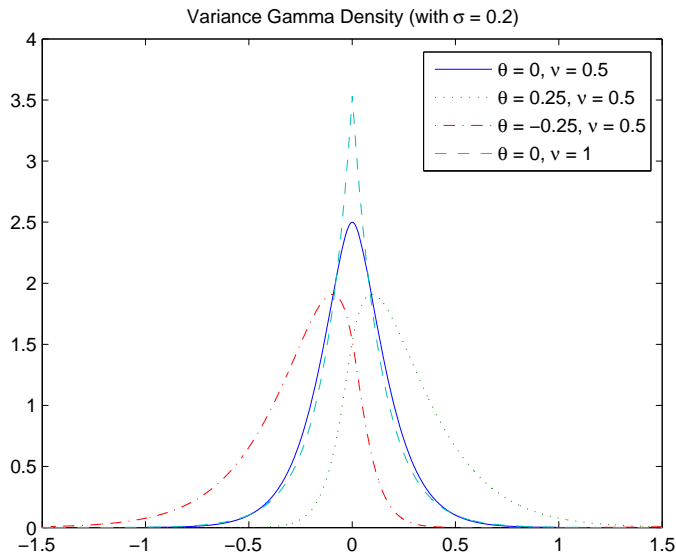


Figure 1.4: Variance Gamma density

Standard moments of $X_{VG}(t)$	
Mean	$\theta t$
Variance	$(\theta^2 \nu + \sigma^2)t$
Skewness	$(2\theta^3 \nu^2 + 3\sigma^2 \theta \nu) / (\theta^2 \nu + \sigma^2)^{3/2} t^{1/2}$
Kurtosis	$3(1 + (\sigma^4 \nu + 4\sigma^2 \theta^2 \nu^2 + 2\theta^4 \nu^3) / (\theta^2 \nu + \sigma^2)^2 t)$

We observe that  $\theta$  is the control parameter for location and skewness,  $\sigma$  is the shape parameter and kurtosis is controlled via  $\nu$  (see Figure 1.4).

Under the mean-corrected risk neutral measure, the asset price is given by:

$$S_t = S_0 \exp(rt + \omega t + X_{VG}(t; \sigma, \nu, \theta)), \quad (1.22)$$

where

$$\omega = \frac{1}{\nu} \ln(1 - \theta \nu - \sigma^2 \nu / 2).$$

We can use another set of parameters  $(C, G, M)$  for the Variance Gamma process, with

$$\begin{aligned} C &= 1/\nu > 0, \\ G &= \left( \sqrt{\frac{1}{4}\theta^2\nu^2 + \frac{1}{2}\sigma^2\nu} - \frac{1}{2}\theta\nu \right)^{-1} > 0, \\ M &= \left( \sqrt{\frac{1}{4}\theta^2\nu^2 + \frac{1}{2}\sigma^2\nu} + \frac{1}{2}\theta\nu \right)^{-1} > 0. \end{aligned}$$

Then the characteristic function is given by:

$$\phi_{\text{VG}}(u, t) = \left( \frac{GM}{GM + (M - G)iu + u^2} \right)^{Ct}. \quad (1.23)$$

The standard moments of  $X_{\text{VG}}(t)$  in terms of  $C$ ,  $G$  and  $M$  are as follows:

Standard moments of $X_{\text{VG}}(t)$	
Mean	$C(G - M)t/MG$
Variance	$C(G^2 + M^2)t/(MG)^2$
Skewness	$2C^{-1/2}(G^3 - M^3)/(G^2 + M^2)^{3/2}t^{1/2}$
Kurtosis	$3(1 + 2C^{-1}(G^4 + M^4)/(M^2 + G^2)^2t)$

Under the mean-corrected risk neutral measure, the asset price is given by:

$$S_t = S_0 \exp(rt + \omega t + X_{\text{VG}}(t; \sigma, \nu, \theta)), \quad (1.24)$$

where

$$\omega = C \ln \left( 1 + \frac{1}{G} - \frac{1}{M} - \frac{1}{GM} \right).$$

### Normal Inverse Gaussian Model

The Normal Inverse Gaussian (NIG) process  $X_{\text{NIG}}(t; \alpha, \beta, \delta)$  is defined as a time-changed Brownian motion with drift:

$$X_{\text{NIG}}(t; \alpha, \beta, \delta) = W(\text{IG}(t; \delta, \sqrt{\alpha^2 - \beta^2}); \beta, \delta).$$

In this case, time  $t$  in the Brownian is changed by a inverse Gaussian process (see Appendix B.2):  $\text{IG}(t; \delta, \sqrt{\alpha^2 - \beta^2})$ . The NIG process has three parameters:  $\alpha > 0$ ,  $-\alpha < \beta < \alpha$  and  $\delta > 0$ .

The density function of  $X_{\text{NIG}}(t)$  is given by:

$$f_{\text{NIG}}(x) = \frac{\alpha\delta}{\pi} \exp(\delta\sqrt{\alpha^2 - \beta^2} + \beta x) \frac{K_1(\alpha\sqrt{\delta^2 + x^2})}{\sqrt{\delta^2 + x^2}}, \quad (1.25)$$

where  $K$  is the modified Bessel function of the second kind (see Appendix B.1). The characteristic function is given by:

$$\phi_{\text{NIG}}(u, t) = \exp[t\delta(\sqrt{\alpha^2 - \beta^2} - \sqrt{\alpha^2 - (\beta + iu)^2})]. \quad (1.26)$$

The standard moments of  $X_{\text{NIG}}(t)$  are as follows:

Standard moments of $X_{\text{NIG}}(t)$	
Mean	$\frac{\delta\beta t}{\sqrt{\alpha^2 - \beta^2}}$
Variance	$\frac{\alpha^2 \delta t}{(\alpha^2 - \beta^2)^{3/2}}$
Skewness	$\frac{3\beta}{\alpha\sqrt{\delta t}(\alpha^2 - \beta^2)^{1/4}}$
Kurtosis	$3\left(1 + \frac{\alpha^2 + 4\beta^2}{\alpha^2 \delta t \sqrt{\alpha^2 - \beta^2}}\right)$

We observe that  $\alpha$  is a shape parameter,  $\beta$  is a skewness parameter and  $\delta$  is a kurtosis parameter (see Figure 1.5).

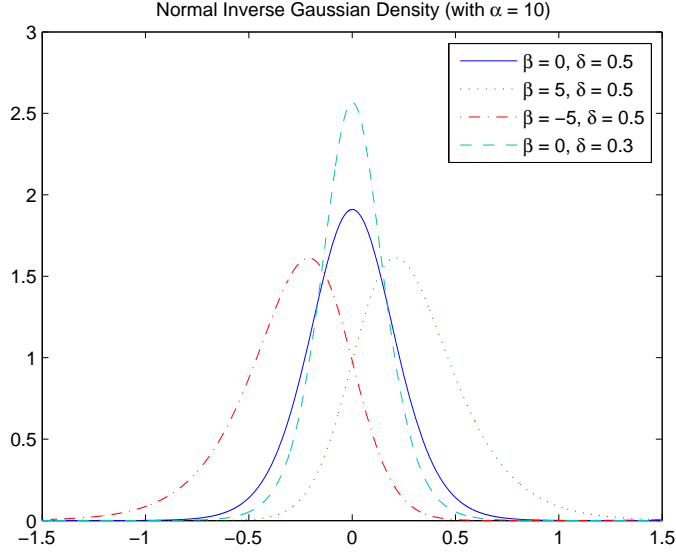


Figure 1.5: Normal Inverse Gaussian density

Under the mean-corrected risk neutral measure, the asset price is given by:

$$S_t = S_0 \exp(rt + \omega t + X_{\text{NIG}}(t; \alpha, \beta, \delta)), \quad (1.27)$$

where

$$\omega = \delta(\sqrt{\alpha^2 - (\beta + 1)^2} - \sqrt{\alpha^2 - \beta^2}).$$

### CGMY Model

The CGMY process  $X_{\text{CGMY}}(t; C, G, M, Y)$  is a four parameter process with  $C > 0$ ,  $G, M \geq 0$  and  $Y < 2$ . When  $Y = 0$ , the CGMY process reduces to the Variance Gamma process  $X_{\text{VG}}(t; C, G, M)$ .

The characteristic function is given by:

$$\phi_{\text{CGMY}}(u, t) = \exp\{tC\Gamma(-Y)[(M - iu)^Y - M^Y + (G + iu)^Y - G^Y]\}. \quad (1.28)$$

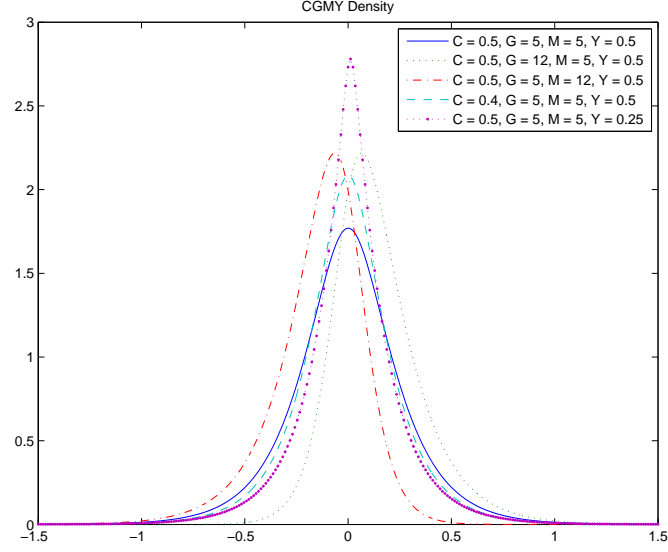


Figure 1.6: CGMY density

The standard moments of  $X_{\text{CGMY}}(t)$  are as follows:

Standard moments of $X_{\text{CGMY}}(t)$	
Mean	$tC(M^{Y-1} - G^{Y-1})\Gamma(1 - Y)$
Variance	$tC(M^{Y-2} + G^{Y-2})\Gamma(2 - Y)$
Skewness	$\frac{C(M^{Y-3} - G^{Y-3})\Gamma(3 - Y)}{t^{1/2}(C(M^{Y-2} + G^{Y-2})\Gamma(2 - Y))^{3/2}}$
Kurtosis	$3 + \frac{C(M^{Y-4} + G^{Y-4})\Gamma(4 - Y)}{t(C(M^{Y-2} + G^{Y-2})\Gamma(2 - Y))^2}$

We observe that the overall arrival rate of jumps is controlled by  $C$ , the parameter  $G$  and  $M$  are the rate of exponential decay on the right and left tails of the Lévy density, lead to skewness of the distribution. The parameter  $Y$  controls the activity rate (see Figure 1.6).

Under the mean-corrected risk neutral measure, the asset price is given by:

$$S_t = S_0 \exp(rt + \omega t + X_{\text{CGMY}}(t; C, G, M, Y)), \quad (1.29)$$

where

$$\omega = -C\Gamma(-Y)[(M-1)^Y - M^Y + (G+1)^Y - G^Y].$$

For the above processes, the characteristic function has an explicit form, so that it is natural to consider the Fourier transform for option pricing. Numerically, the fast Fourier transform (FFT) is a highly accurate and efficient algorithm to implement the Fourier transform and greatly reduces the computational complexity of the discrete Fourier transform (DFT). However, it is restricted to the equally spaced grids. Recently, a more flexible algorithm called the nonequispaced fast Fourier transform (NFFT) has been developed, which enables us to deal with unequally spaced grids. In this thesis, we are going to explore the applications of the NFFT method in option pricing theory. We discuss settings in which this technique can be useful for pricing different types of options, for example, European options, American options and Asian options. It can also be used when the asset follows a wide class of processes, say Lévy processes and mean-reverting processes.

The thesis is organized as follows: In Chapter 2, we will give a review of Fourier transform methods in option pricing and introduce the NFFT approach. In Chapter 3, we consider Asian option pricing. We begin with a review of pricing Asian options including Benhamou [10], and then propose an improved algorithm that uses the NFFT. The accuracy order of the method is also analyzed. In Chapter 4, numerical examples for discrete and continuous Asian options under different underlying distributions are provided, and the convergence rate of our method is demonstrated.

Chapter 5 applies the NFFT method to price European and American options under a wide class of stochastic processes with some kinds of drift based on the semi-Lagrangian method. The class of processes includes some popular mean-reverting processes driven by Brownian motions or Lévy processes, for example the OU process and the CIR process. We conclude and discusses other possible applications of the NFFT in Chapter 6.

## Chapter 2

### An Overview of Fourier Transform Methods

In this chapter, we are going to give an introduction to the Fourier transform. Definitions and basic properties are discussed in Section 2.1. In Section 2.2, we review some literature concerning option pricing by the Fourier transform, and in Section 2.3 the NFFT method is discussed.

#### 2.1 Fourier Transform and Fast Fourier Transform

A sufficiently well-behaved function  $f(t)$  in the time domain can be transformed to a function  $\mathcal{F}(\omega)$  in the frequency domain via the Fourier transform:

$$\mathcal{F}(\omega) = \int_{-\infty}^{\infty} f(t)e^{-i\omega t} dt. \quad (2.1)$$

The inverse transform is given by:

$$f(t) = \frac{1}{2\pi} \int_{-\infty}^{\infty} \mathcal{F}(\omega)e^{i\omega t} d\omega. \quad (2.2)$$

Some important properties of the Fourier transform are listed here:

1. **Time reversal:**  $f(-t) \xleftrightarrow{\mathcal{F}} \mathcal{F}(-\omega)$ .
2. **Time shift:**  $f(t - t_0) \xleftrightarrow{\mathcal{F}} e^{-i\omega t_0} \cdot \mathcal{F}(\omega)$ .
3. **Modulation:**  $e^{-i\omega_0 t} f(t) \xleftrightarrow{\mathcal{F}} \mathcal{F}(\omega - \omega_0)$ .
4. **Convolution:**  $f(t) * g(t) \xleftrightarrow{\mathcal{F}} \mathcal{F}(\omega) \cdot \mathcal{G}(\omega)$ .

5. **Conjugation:**  $\overline{f(t)} \xleftrightarrow{\mathcal{F}} \overline{\mathcal{F}(-\omega)}$ .

6. **Differentiation:**  $f^{(n)}(t) \xleftrightarrow{\mathcal{F}} (i\omega)^n \mathcal{F}(\omega)$ .

7. **Parseval's theorem:**  $\int_{-\infty}^{\infty} f(t) \cdot \overline{g(t)} dt = \int_{-\infty}^{\infty} \mathcal{F}(\omega) \cdot \overline{\mathcal{G}(\omega)} d\omega$ .

In practice, the Fourier transform may need to be approximated by the discrete Fourier transform (DFT), which transforms a complex sequence  $f_j$  into another sequence  $\hat{f}_k \in \mathbb{C}$  via:

$$\hat{f}_k = \sum_{j=-N/2}^{N/2-1} f_j e^{-2\pi i j \frac{k}{N}}, \quad (2.3)$$

where  $k = -\frac{N}{2}, \dots, \frac{N}{2} - 1$ . The inverse discrete Fourier transform (IDFT) is given by:

$$f_j = \frac{1}{N} \sum_{k=-N/2}^{N/2-1} \hat{f}_k e^{2\pi i k \frac{j}{N}}, \quad (2.4)$$

where  $\hat{f}_k$  is the Fourier coefficients and  $j = -\frac{N}{2}, \dots, \frac{N}{2} - 1$ . To connect the Fourier transform and the discrete Fourier transform, we introduce the semidiscrete Fourier transform (see [68] for details). Suppose  $f(t)$  is zero outside the interval  $[-R, R]$ , we think of evaluating the continuous transform (2.1) at  $\omega = k \cdot \frac{\pi}{R}$ ,  $k \in \mathbb{Z}$ , then the semidiscrete Fourier transform is defined by:

$$\hat{f}(k) = \frac{N}{2R} \int_{-R}^R f(t) e^{-ikt \frac{\pi}{R}} dt, \quad (2.5)$$

where  $k \in \mathbb{Z}$ . The inverse semidiscrete Fourier transform is defined by:

$$f(t) = \frac{1}{N} \sum_{k=-\infty}^{\infty} \hat{f}(k) e^{ikt \frac{\pi}{R}}, \quad (2.6)$$

where  $t \in [-R, R]$ . To relate the Fourier transform and the semidiscrete Fourier transform, we periodically copy  $f(t)$  to give  $\bar{f}(t)$ . For  $\bar{f}(t)$ ,  $\mathcal{F}(\omega)$  will be zero unless

$\omega = k \cdot \frac{\pi}{R}$  for some  $k \in \mathbb{Z}$ . For these  $\omega$ ,  $\mathcal{F}(\omega)$  is an infinite sum of Dirac delta distributions centered at  $\omega = k \cdot \frac{\pi}{R}$ . Then  $\mathcal{F}(\omega) = \frac{2R}{N} \cdot \hat{f}(k)$  and the inverse transform generates an infinite sum (2.6). To relate the semidiscrete Fourier transform and the discrete Fourier transform, we let  $t_j = j \cdot \frac{2R}{N}$ ,  $j = -\frac{N}{2}, \dots, \frac{N}{2} - 1$ . By compounded trapezoid rule, we write (2.5) as:

$$\hat{f}(k) = \sum_{j=-N/2}^{N/2-1} f(t_j) e^{-2\pi i j \frac{k}{N}} = \hat{f}_k, \quad (2.7)$$

where  $k = -\frac{N}{2}, \dots, \frac{N}{2} - 1$ . Since  $\hat{f}_{k+N} = \hat{f}_k$ , we have the aliasing relation:  $\hat{f}_k = \sum_{j=-\infty}^{\infty} \hat{f}(k + jN)$ . This is the key to relate the inverse transform and we get:

$$f(t_j) = \frac{1}{N} \sum_{k=-N/2}^{N/2-1} \hat{f}(k) e^{2\pi i k \frac{j}{N}} = f_j, \quad (2.8)$$

where  $j = -\frac{N}{2}, \dots, \frac{N}{2} - 1$ .

The computational complexity of the DFT is  $\mathcal{O}(N^2)$ , so that when  $N$  doubles the computation time increases by four. One way to speed up the computation of the DFT and its inversion is by using the fast Fourier transform (FFT) and the inverse fast Fourier transform (IFFT), for which the computational complexity is only  $\mathcal{O}(N \log N)$  (see [68]). The FFT is a very accurate and efficient numerical method, probably the most important numerical algorithm of the last fifty years. The advantage of using the Fourier transform in option pricing is that the characteristic function of the log-return is just the Fourier transform of the density. If we know the analytical forms of the characteristic functions, we can evaluate the density functions by taking the inverse transform using the FFT. By using the risk-neutral pricing formula, only the density function of the payoff under the risk-neutral measure is needed to compute the option price. Recently, many papers have addressed option

pricing problems via the Fourier transform [10, 17, 20, 25, 32, 45, 54]. One of the earliest was Carr and Madan's method [17] which provides a general way to price options using the Fourier transform. More recently, a convolution method has been presented by Oosterlee et al. [54] to price early exercise options and a Fourier space time-stepping method has been proposed by Jackson et al. [44] to price a wide class of options.

## 2.2 Option Pricing with Fourier Transform

### Carr and Madan's Method

In Carr and Madan's paper [17], they assume that the characteristic function of the log-returns is known analytically. Then they develop an analytical expression for the Fourier transform of the option value. Afterwards, the FFT is used to compute the inverse transform numerically.

Let  $C_T(k)$  be the value of a European call option with maturity  $T$  and strike price  $K$ , they denote  $k = \log K$ ,  $s_T = \log S_T$ , and  $q_T$  the risk-neutral density of  $s_T$ . Then they get:

$$C_T(k) = \int_k^\infty e^{-rT}(e^s - e^k)q_T(s)ds. \quad (2.9)$$

The function  $C_T(k)$  is not square-integrable since  $C_T(k) \rightarrow S_0$  as  $k \rightarrow -\infty$ . However, the Fourier transform and its inversion only work for square-integrable functions (see Plancherel's theorem in [60]). Hence, they consider the modified call price function  $c_T(k)$ :

$$c_T(k) = \exp(\alpha k)C_T(k), \quad (2.10)$$

where  $\alpha > 0$ . Then  $c_T(k)$  is a square-integrable function in  $k$  for some  $\alpha$ . The Fourier

transform of  $c_T(k)$  is defined by:

$$\psi_T(v) = \int_{-\infty}^{\infty} e^{ivk} c_T(k) dk. \quad (2.11)$$

The expression of  $\psi_T(k)$  can be computed directly after an interchange of integrals:

$$\begin{aligned} \psi_T(v) &= \int_{-\infty}^{\infty} e^{ivk} \int_k^{\infty} e^{\alpha k} e^{-rT} (e^s - e^k) q_T(s) ds dk \\ &= \int_{-\infty}^{\infty} e^{-rT} q_T(s) \int_{-\infty}^s (e^{\alpha k+s} - e^{(\alpha+1)k}) e^{ivk} dk ds \\ &= \int_{-\infty}^{\infty} e^{-rT} q_T(s) \left( \frac{e^{(\alpha+1+iv)s}}{\alpha+iv} - \frac{e^{(\alpha+1+iv)s}}{\alpha+1+iv} \right) ds \\ &= \frac{e^{-rT} \phi_T(v - (\alpha+1)i)}{\alpha^2 + \alpha - v^2 + i(2\alpha+1)v}, \end{aligned} \quad (2.12)$$

where  $\phi_T$  is the Fourier transform of  $q_T$ . Note that they need  $\psi_T(0)$  to be finite to ensure  $c_T(k)$  is a square-integrable function. This is equivalent to  $\mathbb{E}(S_T^{\alpha+1}) < \infty$ .

The option price is finally given by the inverse transform of  $\psi_T$ :

$$C_T(k) = \frac{\exp(-\alpha k)}{\pi} \int_0^{\infty} e^{-ivk} \psi(v) dv. \quad (2.13)$$

They apply the FFT to compute this inverse transform as:

$$C_T(k) \approx \frac{\exp(-\alpha k)}{\pi} \sum_{j=0}^{N-1} e^{-iv_j k} \psi(v_j) \eta, \quad (2.14)$$

where  $v_j = \eta j$ ,  $j = 0, \dots, N-1$  and  $\eta$  is the distance between the grid points.

This method is applicable to any underlying processes when the analytical form of the characteristic function of the log-returns is known. Option prices under various models can be derived from this method, for example, Heston's stochastic volatility model [38], Bates's model [9] and exponential Lévy models [62].

## The Convolution Method

In Oosterlee et al. [54], they present an efficient algorithm to price early exercise options, for example American option and Bermudan options. The main idea is to reformulate the risk-neutral pricing formula as a convolution, and the convolution can be computed numerically by the FFT. Their method only requires the characteristic functions of the model, hence it is applicable to general exponential Lévy models.

They define the set of exercise dates as  $T = \{t_1, \dots, t_M\}$  and  $0 = t_0 \leq t_1$ , and assume these dates are equally spaced for simplicity, so that  $t_{m+1} - t_m = \Delta t$ . The price of a Bermudan option can be found via backward induction as

$$\begin{cases} V(t_M, S(t_M)) &= E(t_M, S(t_M)) \\ C(t_m, S(t_m)) &= e^{-r\Delta t} \mathbb{E}[V(t_{m+1}, S(t_{m+1}))] \\ V(t_m, S(t_m)) &= \max\{C(t_m, S(t_m)), E(t_m, S(t_m))\}, \end{cases} \quad (2.15)$$

with  $m = M-1, \dots, 1$ ,  $C$  the continuation value of the option and  $V$  the value of the option immediately before the exercise opportunity.  $E$  denotes the payoff function. Clearly the dynamic programming problem in (2.15) is a successive application of the risk-neutral valuation formula, as they can write the continuation value as

$$C(t_m, S(t_m)) = e^{-r\Delta t} \int_{-\infty}^{\infty} V(t_{m+1}, y) f(y|S(t_m)) dy, \quad (2.16)$$

where  $f(y|S(t_m))$  represents the probability density describing the transition from  $S(t_m)$  at  $t_m$  to  $y$  at  $t_m + 1$ .

The conditional density  $f(y|x)$  in (2.16) only depends on  $x$  and  $y$

$$f(y|x) = f(y - x), \quad (2.17)$$

where  $x$  and  $y$  represent the log price in the exponential Lévy cases. Then the

continuation value can be expressed as

$$C(t_m, x) = e^{-r\Delta t} \int_{-\infty}^{\infty} V(t_{m+1}, x+z) f(z) dz, \quad (2.18)$$

where  $z = y - x$ . (2.18) is just the convolution of  $V(t_{m+1})$  and the conjugate of  $f(z)$ .

They dampen the continuation value (2.18) by a factor  $\exp(\alpha x)$  to ensure the square-integrability and subsequently take its Fourier transform, then they arrive at

$$\begin{aligned} e^{r\Delta t} \mathcal{F}\{c(t_m, x)\}(u) &= \int_{-\infty}^{\infty} \int_{-\infty}^{\infty} e^{iu(x+z)} v(t_{m+1}, x+z) e^{-iz(u-i\alpha)} f(z) dz dx \\ &= \mathcal{F}\{e^{\alpha y} V(t_{m+1}, y)\}(u) \phi(-(u-i\alpha)). \end{aligned} \quad (2.19)$$

where  $c(t_m, x) = e^{\alpha x} C(t_m, x)$ ,  $v(t_m, x+z) = e^{\alpha(x+z)} V(t_m, x+z)$  and  $\phi$  is the extended characteristic function.

Note that  $V(t_M, x) = E(t_M, x)$ , then given  $V(t_{m+1}, x)$ , they can compute  $c(t_m, x)$  and  $C(t_m, x)$  by (2.19) and get  $V(t_m, x) = \max\{E(t_m, x), C(t_m, x)\}$ . American options can be approximated by Bermudan options using small time steps.

### The Fourier Space Time-stepping Method

In Jackson et al. [44], a Fourier transform-based algorithm is presented to price a lot of options under the exponential Lévy models, including European, American, barrier and multi-asset options. They also incorporate regime-switching models into their method. They propose the Fourier time-stepping method to deal with the pricing PIDEs associated with the Lévy processes.

Let  $V(t, S(t))$  be the price of the option at time  $t$ , and

$$v(t, X(t)) = e^{-r(T-t)} V(t, S(0)) e^{X(t)}$$

be the discount-adjusted and log-transformed price process.  $X(t)$  is a Lévy process with triplet  $(\gamma, \sigma^2, \nu)$ . In the exponential Lévy model,  $v$  satisfies the following PIDE:

$$\begin{cases} (\partial_t + \mathcal{L})v &= 0 \\ v(T, x) &= \phi(S(0)e^x), \end{cases} \quad (2.20)$$

where  $\mathcal{L}$  is the infinitesimal generator of the Lévy process and acts on twice-differentiable functions  $f(x)$  as follows (see Section 1.2.2):

$$\mathcal{L}f(x) = \gamma \partial_x f + \frac{1}{2} \sigma^2 \partial_{xx} f + \int_{\mathbb{R}/\{0\}} [f(x+y) - f(x) - y 1_{\{|y|<1\}} \partial_x f(x)] \nu(dy). \quad (2.21)$$

They apply the Fourier transform to the infinitesimal generator  $\mathcal{L}$  of  $X(t)$ , defined by (2.21), then the characteristic exponent of  $X(t)$  can be factored out:

$$\mathcal{F}[\mathcal{L}v](t, \omega) = \Psi(\omega) \mathcal{F}[v](t, \omega), \quad (2.22)$$

where  $\Psi(\omega)$  is the characteristic exponent for a Lévy process given by the Lévy-Khintchine formula. Furthermore, taking the Fourier transform of both sides of the PIDE (2.20) leads to

$$\begin{cases} (\partial_t \mathcal{F}[v](t, \omega) + \Psi(\omega) \mathcal{F}[v](t, \omega) &= 0 \\ \mathcal{F}[v](T, \omega) &= \mathcal{F}[\phi](\omega), \end{cases} \quad (2.23)$$

which is a one-parameter family of ODEs. This is easily solved to find the value at time  $t_1 < t_2$ :

$$v(t_1, x) = \mathcal{F}^{-1} \{ \mathcal{F}[v](t_2, \omega) \cdot e^{(t_2-t_1)\Psi(\omega)} \} (x). \quad (2.24)$$

In the discrete version, letting  $v_m^n = v(t_n, x_m)$  and  $\hat{v}_m^n = \hat{v}(t_n, \omega_m)$ , we have

$$\hat{v}_m^n = \alpha_m \text{FFT}[v^n](m), \quad (2.25)$$

where  $\alpha_m = e^{-i\omega_m x_{min}} \Delta x$ . By taking the inverse transform,

$$v_m^n = \text{FFT}^{-1}[\alpha^{-1} \cdot \hat{v}^n](m). \quad (2.26)$$

Combining these connections between the frequency and spatial domains with the transformed PIDE (2.23), a step backwards in time is computed by

$$v^{n-1} = \text{FFT}^{-1}[\text{FFT}[v^n] \cdot e^{\Psi \Delta t}]. \quad (2.27)$$

Based on this Fourier time-stepping method, Jackson et al. are able to compute European, American, barrier and shout options. Multi-asset problems and regime-switching cases are also discussed in their paper.

### 2.3 Nonequispaced Fast Fourier Transform

In this thesis, we are going to highlight situations in which the Fourier methods might be appropriate, but where the FFT cannot be used, and the computational efficiency it offers is lost. This happens when we need to evaluate the Fourier transform at a given unequally spaced grid. The nonequispaced fast Fourier transform (NFFT) is a generalization of the standard FFT to evaluate a trigonometric polynomial at a set of arbitrary points  $x_j$ ,  $j = 0, \dots, M - 1$  efficiently (but approximately):

$$f(x_j) = \sum_{k=-N/2}^{N/2-1} \hat{f}_k e^{-2\pi i k x_j}. \quad (2.28)$$

The computational complexity of the method is  $\mathcal{O}(N \log N + M \log(1/\varepsilon))$ , where  $\varepsilon$  is the desired accuracy. It is obvious that if we consider equispaced nodes  $x_j = \frac{j}{N}$ ,  $j = -\frac{N}{2}, \dots, \frac{N}{2} - 1$ , (2.28) reduce to the standard DFT (2.3) which can be computed by the FFT.

Recently, some papers address the problem of fast computing this discrete Fourier transform on unequally spaced grid through various techniques. For example, the Taylor expansion [5], Lagrange interpolation [27], local Chebyshev approximation [66], translates of Gaussian bells [65], etc. Among them, the Taylor expansion approach is a simple but fast scheme to compute (2.28), the nonequispaced discrete Fourier transform (NDFT). In this approach, provided unequally spaced nodes  $x_j \in [-\frac{1}{2}, \frac{1}{2})$ , we need the nearest neighboring nodes on an over-sampled equally spaced grid  $\{n^{-1}k - \frac{1}{2}\}_{k=0, \dots, n-1}$  where  $n = \sigma N$  and  $\sigma$  is called the over-sampling factor,  $\sigma > 1$ . We use  $m$ th order Taylor expansion of this trigonometric polynomial about this equally spaced grid. Then we apply the standard FFT on this  $n$  points equally spaced grid  $m$  times to get the approximation of  $f(x_j)$  in (2.28).

$$\begin{aligned} f(x_j) &= \sum_{k=-N/2}^{N/2-1} \hat{f}_k e^{-2\pi i k x_j} \\ &= \sum_{k=-N/2}^{N/2-1} \hat{f}_k e^{-2\pi i k (x_j - \lfloor x_j \rfloor)} e^{-2\pi i k \lfloor x_j \rfloor}. \end{aligned} \quad (2.29)$$

We just apply Taylor expansion on  $e^{-2\pi i k (x_j - \lfloor x_j \rfloor)}$  in (2.29). The computational complexity is  $\mathcal{O}(N \log N + M)$ .

Another efficient approach which is used to implement the NFFT in this thesis is by special linear combinations of translates of suitable window functions  $\varphi$ , say a Gaussian bell [65]. Set  $n = \sigma N$ , and  $\sigma$  is still the over-sampling factor with  $\sigma > 1$ . Let  $\varphi$  be a 1-periodic continuous function with bounded variation. Steidl in [65] approximates  $f$  in (2.28) by

$$s_1(x) = \sum_{l=-n/2}^{n/2-1} g_l \varphi \left( x - \frac{l}{n} \right). \quad (2.30)$$

Since  $\varphi$  is well-localized in the time domain, it can be approximated by a 1-periodic function  $\psi$ ,

$$\psi(x) = \varphi(x)1_{[-\frac{m}{n}, \frac{m}{n}]}(x), \quad (2.31)$$

where  $m < n$ ,  $m \in \mathbb{N}$ . Denote  $\hat{\varphi}(k)$  and  $\hat{g}_k$  as the Fourier coefficients of  $\varphi(x)$  and  $g_l$ ,  $k = -N/2, \dots, N/2 - 1$ , the algorithm is summarized here.

1. Compute  $\hat{\varphi}(k)$ ,  $k = -N/2, \dots, N/2 - 1$  and  $\psi(x_j - l/n)$ ,  $j = 0, \dots, M - 1$ ,  $l = \lfloor nx_j \rfloor - (m - 1), \dots, \lceil nx_j \rceil + (m - 1)$ .

2. Compute  $\hat{g}_k$  with

$$\hat{g}_k = \begin{cases} f_k/\hat{\varphi}(k), & k = -N/2, \dots, N/2 - 1. \\ 0, & k = -n/2, \dots, -N/2 - 1; k = N/2, \dots, n/2 - 1. \end{cases}$$

3. Compute  $g_l$ ,  $l = -n/2, \dots, n/2 - 1$  by the standard FFT

$$g_l = \frac{1}{n} \sum_{k=-N/2}^{N/2-1} \hat{g}_k e^{-2\pi i k l / n}.$$

4. For  $j = 0, \dots, M - 1$ , compute  $s(x_j)$  to approximate  $f(x_j)$ .

$$s(x_j) = \sum_{l=-n/2}^{n/2-1} g_l \psi(x_j - \frac{l}{n}).$$

The computational complexity of this algorithm is  $\mathcal{O}(N \log N + M)$ .

If a Gaussian bell is used as the function  $\varphi$ ,

$$\varphi(x) = \frac{1}{\sqrt{\pi b}} \sum_r e^{-(n(x+r))^2/b}, \quad (2.32)$$

and

$$\psi(x) = \frac{1}{\sqrt{\pi b}} \sum_r e^{-(n(x+r))^2/b} 1_{(-m, m)}(n(x+r)), \quad (2.33)$$

with  $1 \leq m < n/2$ ,  $1 \leq b \leq \frac{2\sigma m}{(2\sigma-1)\pi}$ , then the error of  $|f(x_j) - s(x_j)|$  is given by

$$E \leq 4\|f\|_1 e^{-b\pi^2(1-1/\sigma)}. \quad (2.34)$$

Details about other approaches to implement the NFFT and the comparison of these approaches can be found in [46, 55, 72].

## Chapter 3

### Pricing Asian Options via the NFFT

In this chapter, we propose an efficient algorithm for pricing Asian options based on the nonequispaced fast Fourier transform (NFFT). In the first section, we will give an overview of some popular methods for Asian option pricing, including Vercher's PDE approach [70], Monte Carlo simulation [49] and Benhamou's FFT method [10]. The details about our pricing algorithm which improves the efficiency of Benhamou's method by introducing the NFFT are discussed in Section 3.2. The error analysis of our method and Benhamou's method is provided in Section 3.3.

#### 3.1 An Overview of Pricing Asian Options

Originally introduced in Tokyo, Asian options are among the most popular path-dependent options traded in exchanges and over-the-counter markets. The payoff of an Asian option depends on the arithmetic average of the underlying asset price, for example, interest rates, indices and commodities, over a certain period of time. This averaging feature makes Asian options less volatile than the European options on their underlying asset. In addition, the price of Asian options is less sensitive to possible spot price manipulations. Therefore, Asian options are often cheaper than standard derivatives on the same underlying and provide the investors with a good choice to hedge their positions in the market.

In terms of the price of the Asian option, no exact closed-form solutions are

available even in the classic geometric Brownian motion case. This is due to the fact that there is no explicit formula for the distribution of the arithmetic average of log-normal random variables. In this case, a variety of numerical methods and approximations have been developed in the literature to evaluate Asian options:

- Tree methods (Hull and White [42], Hsu and Lyuu [41]),
- Monte Carlo simulation (Kemna and Vorst [47], Lapeyre and Temam [49]),
- Partial differential equation (Forsyth, Vetzal and Zvan [29], Vecer [70]),
- Laplace and Fourier transforms (Geman and Yor [34], Benhamou [10]),
- Approximate analytic methods (Rogers and Shi [58], Thompson [67]).

In the following, I will discuss some of these approaches used in pricing Asian options. These include the PDE approach proposed by Vecer [70], the Monte Carlo simulation by Lapeyre and Temam [49], and the fast Fourier transform (FFT) method by Benhamou [10]. The advantages and drawbacks of these methods are also discussed.

Under the risk neutral measure  $\mathbb{Q}$ , we assume that the dynamics of the underlying asset price is given by the following SDE:

$$dS_t = rS_t dt + \sigma S_t dW_t,$$

where  $S_t$  is the spot price at time  $t$ ,  $W_t$  is a Brownian motion,  $r$  and  $\sigma$  stand for the risk free rate and volatility respectively.

The general payoff of an Asian option can be expressed as:

$$f = (A - K_1 S_T - K_2)^+ \text{ or } f = (K_2 - K_1 S_T - A)^+,$$

where  $A$  is the average of the asset price. In the continuous case,  $A = \frac{1}{T} \int_0^T S_t dt$ , and in the discrete case,  $A = \frac{1}{n+1} \sum_{i=0}^n S_{t_i}$ . Moreover, when  $K_1 = 0$ , we have the fixed strike Asian option, when  $K_2 = 0$ , we have the floating strike Asian option.

According to the risk neutral pricing formula, the price of an Asian option can be written as:

$$V(0, S_0, K_1, K_2) = e^{-rT} \mathbb{E}^{\mathbb{Q}}[f(A, S_T, K_1, K_2)].$$

To evaluate this, we usually need to find the density of the average  $A$  numerically.

### 3.1.1 The PDE method

Vecer [70] provides a unifying approach for pricing Asian options, for both discrete and continuous arithmetic average. Moreover, this approach easily incorporates cases of continuous or discrete dividends, and floating or fixed strike. The idea is to replicate the price average by self-financing trading in the underlying asset, and the resulting one-dimensional PDE for the price of the Asian option can be easily implemented to give extremely fast and accurate results.

He assume that the stock price has the following dynamics under the risk-neutral measure:

$$dS_t = S_t(rdt - d\nu_t + \sigma dW_t),$$

where  $r$  is the interest rate,  $\sigma$  is the volatility and  $\nu_t$  is the measure representing the dividend yield. For example, when  $\nu_t = \gamma dt$ , we have a continuous dividend yield at the rate  $\gamma$ .

Suppose that he want to price a option whose payoff depends on  $\int_0^T S_t d\mu(t)$ , where  $\mu(t)$  represents a general weighting factor. For continuous averaging he had

$d\mu(t) = \frac{1}{T}dt$ , for discrete averaging ( $n$  points) he set

$$d\mu(t) = \frac{1}{n} \sum_{k=1}^n \delta\left(\frac{k}{n}T\right) dt,$$

so that  $\int_0^T S_t d\mu(t)$  becomes the discrete average,  $\frac{1}{n} \sum_{k=1}^n S_{\frac{k}{n}T}$ . Here  $\delta(\cdot)$  is the Dirac delta function.

In order to replicate the payoff, he find a trading strategy  $q_t$  such that the wealth at maturity  $X_T$  satisfies:

$$X_T = \int_0^T S_t d\mu(t) - K_2.$$

By Itô's lemma, the trading strategy  $q_t$  turns out to be:

$$q_t = \exp\left(-\int_t^T d\nu(s)\right) \cdot \int_t^T \exp\left(-r(T-s) + \int_s^T d\nu(s)\right) d\mu(s). \quad (3.1)$$

Therefore, the price of the Asian option with the payoff  $(\int_0^T S_t d\mu(t) - K_1 S_T - K_2)^+$  on a stock paying arbitrary dividends at the rate  $d\nu_t$  is given by

$$V(0, S_0, K_1, K_2) = S_0 \cdot u(0, Z_0), \quad (3.2)$$

where  $u(t, z)$  satisfies

$$u_t + \frac{1}{2} \left(z - e^{-\int_0^t d\nu(s)} q_t\right)^2 \sigma^2 u_{zz} = 0 \quad (3.3)$$

$$u(T, z) = (z - K_1)^+. \quad (3.4)$$

The strategy  $q_t$  is given by (3.1) and  $Z_0 = \frac{X_0}{S_0} = q_0 - e^{-rT} \frac{K_2}{S_0}$ .

This pricing method is flexible to deal with both continuous and discrete type of Asian options with either floating or fixed strike, by choosing specific  $d\mu(t)$ ,  $K_1$  and  $K_2$ . In addition, the numerical experiment in [70] shows that the method is stable for all choices of parameters (even for small volatilities and short maturities) and gives accurate results within 6 decimal digits in less than a second of computation time.

### 3.1.2 The Monte Carlo method

The Monte Carlo simulation was introduced to option pricing by Boyle [14]. Although this method is generally not an efficient way to price Asian options, Lapeyre and Temam in [49] show that, with a carefully chosen scheme and variance reduction techniques, it becomes a competitive algorithm for Asian options under some circumstances.

In order to price an Asian option, they have to simulate the average of the stock price, denoted by  $A = \frac{1}{T} \int_0^T S_t dt$ . In [49], they present two high accuracy schemes to simulate this average.

They divided the interval  $[0, T]$  into  $n$  steps with step size  $h = T/n$ , and define the time nodes  $t_k = kT/n = kh$ ,  $k = 0, \dots, n$ . In the first scheme, they use  $\mathbb{E}(\frac{1}{T} \int_0^T S_t dt | \mathcal{F})$  as the approximation to the average  $A$ , where  $\mathcal{F}$  is the  $\sigma$ -field generated by  $(S_{t_k}, k = 0, \dots, n)$ . They show that this does not lose any accuracy. Then they express it as a function of  $W_{t_k}$ :

$$\mathbb{E} \left( \frac{1}{T} \int_0^T S_t dt | \mathcal{F} \right) = \frac{1}{T} \sum_{k=0}^{n-1} \int_{t_k}^{t_{k+1}} e^{\sigma \frac{t-t_k}{h} (W_{t_{k+1}} - W_{t_k}) - \frac{\sigma^2}{2} \frac{(t-t_k)^2}{h} + rt} e^{\sigma W_{t_k} - \frac{\sigma^2}{2} t_k} dt. \quad (3.5)$$

In the Monte Carlo simulation, this approximation is used in a double loop (in times and in the number of simulation), so it is really necessary to simplify this formula. Hence, a formal Taylor expansion can be done with  $h$  small, which leads to a more practical scheme:

$$A = \frac{h}{T} \sum_{k=0}^{n-1} S_{t_k} \left( 1 + \frac{rh}{2} + \sigma \frac{W_{t_{k+1}} - W_{t_k}}{2} \right). \quad (3.6)$$

Another similar scheme can be obtained by the fact that the Brownian motion is

a Gaussian process so that  $\int_0^T W_t dt$  can be easily simulated. Hence,

$$A = \frac{1}{T} \sum_{k=0}^{n-1} S_{t_k} \int_{t_k}^{t_{k+1}} e^{\sigma(W_t - W_{t_k}) - \frac{\sigma^2}{2}(t - t_k) + r(t - t_k)} dt. \quad (3.7)$$

Using a Taylor expansion again, we obtain the following scheme:

$$A = \frac{1}{T} \sum_{k=0}^{n-1} S_{t_k} \left( h + \frac{rh^2}{2} + \sigma \int_{t_k}^{t_{k+1}} (W_t - W_{t_k}) dt \right). \quad (3.8)$$

The efficiency of these two schemes (3.6) and (3.8) was demonstrated by a favorable rate of convergence at  $\frac{1}{n}$  and  $\frac{1}{n^{3/2}}$  respectively. In addition, the variance reduction techniques developed by Kemna and Vorst [47] can be used to increase the efficiency of the simulation and improve the convergence of these two schemes. Compared with the tree method by Hull and White [42], the numerical examples in [49] demonstrate that the Monte Carlo simulation under these schemes is more efficient when higher accuracy, say 4 decimal digits, is required.

### 3.1.3 The FFT Method

The fast Fourier transform (FFT) was first used in Asian option evaluation by Caverhill and Clewlow [18] and an improved version of their method was developed by Benhamou [10] to price discrete Asian options by recentering the intermediate densities, so that the grid size and the computational time are both reduced. This method was also adapted to the cases of non-lognormal densities in his paper.

The part of his method involving the FFT is to compute the density of the arithmetic average  $A = \frac{1}{n+1} \sum_{i=0}^n S_{t_i}$ . Here he define the log return series  $(R_{t_i})_{i \in \mathbb{N}}$  by  $R_{t_i} = \log(S_{t_i}/S_{t_{i-1}})$  and the mean of  $R_{t_i}$  by  $\mu_i$ . Then he introduce the following two sequences  $(m_i)_{i=1 \dots n}$  and  $(A_i)_{i=1 \dots n}$  with initial values:  $m_1 = \mu_n$  and  $A_1 = R_{t_n} - m_1$ ,

for  $i = 2 \dots n$

$$m_i = \mu_{n+1-i} + \log(1 + \exp m_{i-1}), \quad (3.9)$$

and

$$A_i = R_{t_{n+1-i}} + \log(1 + \exp(A_{i-1} + m_{i-1})) - m_i. \quad (3.10)$$

The sequence  $(m_i)_{i=1\dots n}$  acts as a proxy for the mean of the recursive sequence used in [18], and therefore  $(A_i)_{i=1\dots n}$  is called the recentered sequence. In this case, the average  $A$  can be expressed as:

$$A = \frac{S_{t_0}}{n+1} (1 + e^{A_n + m_n}). \quad (3.11)$$

To compute the density of  $A$ , the algorithm starts with the value of the two dimensional sequence  $m_1$  and  $A_1$  and finishes when he get  $m_n$  and  $A_n$ . By the definition of  $m_i$ ,  $A_i$  is centered at each step and hence only a small grid is need for the algorithm.

The recursive sequence is calculated as follows. Assume  $m_{i-1}$  and  $A_{i-1}$  are known:

- He then interpolate the variable  $A_i$  by the following formula to get the density of the variable  $\log(1 + e^{m_{i-1} + A_{i-1}}) - m_i$ :

$$dp_{\log(1+e^{m_{i-1}+X})-m_i}(y) = \frac{e^{y+m_i}}{e^{y+m_i} - 1} p_X(\log(e^{y+m_i} - 1) - m_{i-1}) 1_{\{y > -m_i\}} dy. \quad (3.12)$$

- He calculate the density of  $A_i$  as the sum of the two independent variable  $R_{t_{n+1-i}}$  and the variable  $\log(1 + e^{m_{i-1} + A_{i-1}}) - m_i$  by calculating the convolution product via the FFT.

After obtaining the density of  $A_n$ , he compute the density of the average, and then calculate the payoff of the Asian option, defined as an expectation under the risk neutral measure, by a numerical integration.

His algorithm can be summarized in Algorithm 1 and in the following graph:

---

**Algorithm 1** Asian options via the interpolation

---

1. Choose a fine grid  $[-w, w]$  with  $N$  points.
  2. Compute  $m_i$  and evaluate  $f_{R_{t_i}}$  on the grid.
  3. Evaluate  $f_{A_1}$  on the grid.
  4. Loop  $i = 2$  to  $n$ . **Input:**  $f_{A_{i-1}}$ .
    - Evaluate  $f_{g(A_{i-1})}$  on the grid via the cubic interpolation.
    - $f_{A_i} = f_{R_{t_{n+1-i}}} * f_{g(A_{i-1})}$ .
 End Loop. **Output:**  $f_{A_i}$ .
  5. Compute the price  $P$  by Trapezoid rule or Simpson's rule.
- 

$$\text{Real space: } f_{A_{i-1}} \xrightarrow{\text{Interpolation(3.12)}} f_{g(A_{i-1})} \xrightarrow{\text{Convolution}} f_{A_i}$$

According to Benhamou's method, if we plot the evolution of the probability density of  $A_i$ , we shall find that the densities are centered at each step. Figure 3.1 shows the plot of the evolution for 20 steps.

It is shown that recentering the density improved significantly the efficiency of the FFT method especially for high volatilities in the log-normal case. In fat-tailed distributions, this method also works efficiently and provides a more expensive price for the Asian option. We can conclude that the FFT method is efficient for discrete Asian option pricing, which is consistent with any type of underlying densities, especially non-lognormal returns. Hence, the method can be easily extended to the exponential Lévy models.

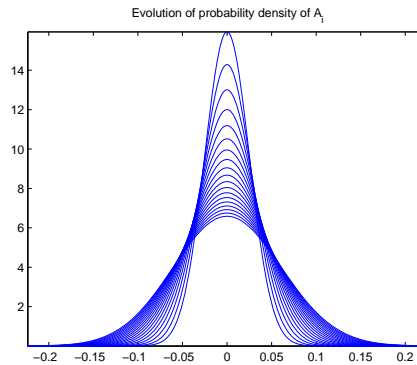


Figure 3.1: The evolution of the probability density

Although it is a good way to price Asian options, there are three aspects can be modified so that the performance and the convergence rate of the algorithm will be highly improved. (i) The chosen width of the grid is too big, so that more grid points are needed to ensure the accuracy. (ii) We can make the algorithm work in the Fourier space, i.e. using the explicit form of characteristic functions directly. Then we could replace the time cost convolution with the multiplication of the Fourier coefficients. This make more sense when the analytical form of the density function is not available or is complicated. (iii) The convergence of the interpolation is rather slow, which can be replaced by the highly efficient nonequispaced fast Fourier transform (NFFT) method. To take advantage of the NFFT, high accuracy numerical integration methods, for example, Gaussian quadrature and Romberg integration, are needed to compute the final expectation (see Appendix A.3).

The algorithm incorporating such aspects will be fully discussed in the following section, and the efficiency of the algorithm will be demonstrated by error analysis in Section 3.3 and by some numerical examples in Chapter 4.

### 3.2 NFFT Algorithm for Asian Options

From Benhamou's interpolation algorithm, we know that the average  $A$  can be represented as (3.11). We will propose a different recursive algorithm to compute the density of the average  $A$  via the NFFT. We will use the characteristic functions directly and switch between the Fourier space and the real space. To start with, we need to determine the grid by choosing its width, denoted by  $[-w, w]$  and the number of the grid points, denoted by  $N$ . The width should be chosen large enough to cover the support of the densities at each step and the number  $N$  should be large enough to keep the accuracy. The following algorithm is run on this fixed grid:

- Compute the sequence  $(m_i)_{i=1\dots n}$  by (3.9), so that the densities of  $A_i$  are centered.
- Evaluate the characteristic function of  $R_{t_i}$  at the corresponding grid points. In the log-normal case, the characteristic function of the log-return is given by

$$\phi_R(u) = e^{iu(r - \frac{\sigma^2}{2})\Delta t - \frac{\sigma^2 u^2}{2}\Delta t}.$$

- Evaluate the characteristic function of  $A_1$  at the corresponding grid points, where  $A_1 = R_{t_n} - m_1$ .

Given the characteristic function of  $A_{i-1}$  at the corresponding grid, we compute the characteristic function of  $A_i$  at that grid. It ends when we get the characteristic function of  $A_n$ . We repeat the following:

- Given the characteristic function of  $A_{i-1}$ , evaluate the characteristic function of the variable  $\log(1 + e^{A_{i-1} + m_{i-1}}) - m_i$  at the determined grid points (evenly-

spaced grid). Let  $Y = g_i(A_{i-1}) = \log(1 + e^{A_{i-1} + m_{i-1}}) - m_i$ , we do the following steps:

1. Find the grid points  $y_k$  where the inverse function  $g_i^{-1}(x)$  exists, that is, the grid points  $y_k > -m_i$ .
2. Deduce the unevenly-spaced grid of  $A_{i-1}$  by  $x_k = g_i^{-1}(y_k)$ , but we only use those points inside the fixed grid  $[-w, w]$  as our objective unevenly-spaced grid.
3. Evaluate the density of  $A_{i-1}$  at the above unevenly-spaced points by applying the NFFT to the characteristic function of  $A_{i-1}$ , and pad zeros at the points outside the fixed grid.
4. Evaluate the density of  $Y = g_i(A_{i-1})$  at the points  $y_k$  by

$$f_Y(y_k) = \left| \frac{1}{g'(x_k)} \right| f_{A_{i-1}}(x_k),$$

and pad zeros at other points on the fixed grid.

5. Compute the characteristic function of  $Y = g_i(A_{i-1})$  by the IFFT.

$$\phi_Y(u_j) = 2w \frac{1}{N} \sum_{k=-N/2}^{N/2-1} f_Y(y_k) e^{2\pi i j \frac{k}{N}}, j = -N/2 \dots N/2 - 1.$$

- Compute the characteristic function of  $A_i$  by multiplying the characteristic function of  $Y$  and the characteristic function of  $R_{t_{n+1-i}}$  on the grid.
- After obtaining the density of  $A_n$ , we calculate the payoff of the Asian option by a careful numerical integration.

At the final stage, we have the density of  $A_n$  and need to calculate the following:

$$P = e^{-rT} \mathbb{E}^{\mathbb{Q}}[(A - K)_+], \quad (3.13)$$

where

$$A = \frac{S_0}{n+1}(1 + e^{A_n+m_n}).$$

If we are not careful in computing this integral, we may lose some accuracy offered by the Fourier transform. We could express this expectation in terms of the density function of  $A_n$ :

$$\begin{aligned} & e^{-rT} \mathbb{E}^{\mathbb{Q}}[(A - K)_+] \\ &= e^{-rT} \mathbb{E}^{\mathbb{Q}} \left[ \left( \frac{S_0}{n+1}(1 + e^{A_n+m_n}) - K \right)_+ \right] \\ &= e^{-rT} \int_{-\infty}^{\infty} \left[ \frac{S_0}{n+1}(1 + e^{x+m_n}) - K \right]_+ f_{A_n}(x) dx \\ &= e^{-rT} \int_{x_0}^{\frac{w}{2}} \left[ \frac{S_0}{n+1}(1 + e^{x+m_n}) - K \right] f_{A_n}(x) dx \end{aligned} \quad (3.14)$$

where

$$x_0 = \log \left[ \frac{(n+1)K}{S_0} - 1 \right] - m_n.$$

Now the non-smooth integrand is changed to a smooth one. Then we can apply either Gaussian quadrature or Romberg integration (see Appendix A.3) to compute this integral. For Gaussian quadrature, we just input the limits of the integral  $x_0$  and  $w/2$ , then output the new Gaussian grid  $\tilde{x}_i$  and weights  $w_i$  with  $i = 1 \dots n$ ,  $n$  is the degree of the Legendre polynomial. Since we know the values of the characteristic function of  $A_n$ , which are the Fourier coefficients of the density, we can apply the NFFT to evaluate the density on the Gaussian grid points  $\tilde{x}_i$ . For Romberg integration, we can also use the NFFT to evaluate the density on the Romberg grid on  $[x_0, w/2]$  with  $2^N$  points.

The algorithm can be illustrated in Algorithm 2 and in the following graph. The computational complexity of this algorithm is  $\mathcal{O}(2nN \log N + nM)$ , where  $M$  is the

number of unevenly-spaced points.

---

**Algorithm 2** Asian options via the NFFT

---

1. Choose a fine grid  $[-w, w]$  with  $N$  points.
  2. Compute  $m_i$  and  $\phi_{R_{t_i}}(u)$ .
  3. Compute  $\phi_{A_1}(u)$ .
  4. Loop  $i = 2$  to  $n$ . **Input:**  $\phi_{A_{i-1}}(u)$ .
    - Deduce the unevenly-spaced grid by taking  $g^{-1}(x)$ .
    - Evaluate  $f_{A_{i-1}}$  on the unevenly-spaced grid via the NFFT.
    - Evaluate  $f_{g(A_{i-1})}$  on the evenly-spaced grid.
    - Compute  $\phi_{g(A_{i-1})}(u)$  by the IFFT.
    - $\phi_{A_i}(u) = \phi_{R_{t_i}}(u) \cdot \phi_{g(A_{i-1})}(u)$ .
 End Loop. **Output:**  $\phi_{A_i}(u)$ .
  5. Compute  $P$  by Gaussian quadrature or Romberg Integration.
- 

$$\begin{array}{ccc}
 \text{Fourier space:} & \phi_{A_{i-1}} & \xrightarrow{\quad} \phi_{g(A_{i-1})} \longrightarrow \phi_{A_i} \\
 & \text{NFFT} \downarrow & \uparrow \text{IFFT} \\
 \text{Real space:} & f_{A_{i-1}}(\text{uneven}) & \xrightarrow{f_Y(y) = \left| \frac{1}{g'(x)} \right| f_{A_{i-1}}(x)} f_{g(A_{i-1})}(\text{even})
 \end{array}$$

The method is flexible to incorporate floating rate strike Asian options, put style options and options with dividend payments. Besides, it is also able to deal with arbitrary piecewise smooth payoffs.

### 3.3 Error Analysis

In this section, we analyze the errors of Benhamou's interpolation method and our NFFT algorithm including various numerical integration techniques that are used. This analysis will demonstrate why the NFFT is a good candidate here and why it offers a high rate of convergence.

There are many ways to compute a integral  $\int_a^b f(x)dx$  numerically. The methods used in this thesis include trapezoid rule, Simpson's rule, Gaussian quadrature and Romberg integration. The details about these methods can be found in [48]. Assume that we have chosen an equally spaced grid with  $N + 1$  points,  $[x_0, x_1, \dots, x_{N-1}, x_N]$ , where  $x_0 = a$ ,  $x_N = b$  and  $x_i = x_0 + ih$ ,  $i = 1, 2, \dots, N$ ,  $h = \frac{b-a}{N}$ . The error term of the trapezoid rule is given by

$$E_N = -\frac{1}{12}(b-a)h^2 f''(\xi), \quad (3.15)$$

where  $\xi \in (a, b)$ . Hence, its order of error is  $\mathcal{O}(h^2)$  or  $\mathcal{O}(N^{-2})$ , which means the quadratic convergence of the trapezoid rule. For Simpson's rule, the error term is

$$E_N = -\frac{1}{180}(b-a)h^4 f^{(4)}(\xi), \quad (3.16)$$

where  $\xi \in (a, b)$ . Obviously, the order of error is  $\mathcal{O}(h^4)$ . For  $n$  points Gaussian quadrature, the error term of Gaussian-Legendre one is

$$E_n = \frac{2^{2n+1}(n!)^4}{(2n+1)[(2n)!]^3} f^{(2n)}(\xi), \quad (3.17)$$

where  $\xi \in (a, b)$ . The order of error is just  $\mathcal{O}\left(\frac{2^{2n+1}(n!)^4}{(2n+1)[(2n)!]^3}\right)$ . Here,  $n$  is the number of Gaussian points, not our original grid points. For Romberg integration with  $2^n$  grid points, the order of error is  $\mathcal{O}\left(h_n^{2^{(n+1)}}\right)$ . Obviously, the Romberg integration and Gaussian quadrature can achieve very high accuracy with enough points.

In terms of the interpolation, the error term of degree  $N$  polynomial interpolation is given by:

$$E_N = \frac{1}{(N+1)!} f^{(N+1)}(\xi) \prod_{i=0}^N (x - x_i), \quad (3.18)$$

where  $\xi \in (a, b)$ . If we perform the linear interpolation piecewise on the above grid, i.e.  $N = 1$ , then the error is bounded by  $\frac{1}{2}h^2 f''(\xi)$  and the order of error is obviously

$\mathcal{O}(h^2)$  or  $\mathcal{O}(N^{-2})$ , the same as the trapezoid rule. If we use cubic spline interpolation or cubic Hermite interpolation, the error is bounded by  $\frac{5}{384}h^4 f^{(4)}$  and  $\frac{1}{384}h^4 f^{(4)}$  respectively. This means we have the order of error at  $\mathcal{O}(h^4)$ , the same as the Simpson's rule. That's why Benhamou uses Simpson's rule to compute the integration at the end. Therefore, if we apply the interpolation together with the trapezoid rule, the order of accuracy of the algorithm is just  $\mathcal{O}(N^{-2})$ , which is restricted by the trapezoid rule. If we use the cubic interpolation, the order of accuracy of the algorithm is at most  $\mathcal{O}(N^{-4})$ . No matter how accurately the final numerical integration is performed, the overall accuracy will not be improved. Hence, if we need to attain  $d$  digits accuracy, we have to use  $\mathcal{O}(e^{d/4})$  sample points.

As for the FFT, if  $f$  is a periodic function with its derivatives up to order  $s$ , then the error of the FFT is bounded by

$$E \leq CN^{-s} \|f\|_s, \quad (3.19)$$

where  $C$  is a constant. If  $f$  has infinitely many continuous derivatives, then (3.19) is true for every  $s \geq 0$ . If  $f$  is suitably analytic, it may even attain a faster rate of convergence at  $\mathcal{O}(e^{-CN})$ , which implies the exponential accuracy of the FFT. In the implementation of the NFFT by using a Gaussian bell as discussed in Section 2.3, besides the error of the FFT, there is an extra approximation error at  $\mathcal{O}(e^{-b\pi^2(1-1/\sigma)})$  (2.34). If the cut off parameter  $m$  and the over-sampling factor  $\sigma$  are chosen properly so that  $b$  is large enough, the NFFT will also attain the exponential accuracy. Hence, we can make use of those high accurate numerical integration, Gaussian quadrature or Romberg integration, with enough integration points to guarantee the exponential accuracy of the algorithm. This is what gives the faster convergence of our algorithm.

If we have the order of accuracy at  $\mathcal{O}(e^{-CN})$ , then we only need  $\mathcal{O}(d)$  sample points to get  $d$  accurate digits. Compared with the interpolation method, we can use far fewer sample points in the NFFT approach to get same accurate digits, or say we can use the same number of points in the NFFT to get more digits than the interpolation.

Numerical examples of pricing Asian options via our NFFT algorithm and the convergence of different methods will be provided in the next chapter.

## Chapter 4

### Numerical Examples

In this chapter, we will present some numerical examples of the implementation of the algorithm introduced in Chapter 3 for pricing Asian options based on the NFFT. The efficiency of this algorithm together with its rate of convergence are also discussed. In the second section, an extension of this algorithm to the continuous case is given. In the third section, we compare the results in some popular Lévy models with the log-normal model.

All the examples in this thesis are performed in Matlab 7.4.0 on an Intel Pentium M 760, 2.0GHz CPU with 1G DDR2 SDRAM.

#### 4.1 Asian Options under the Log-normal Model

We just use the same example as in the paper of Benhamou [10] to illustrate our algorithm for pricing Asian options. We compute the price of a one year weekly Asian option ( $T = 1$ ), with the number of observation dates  $n = 50$ , the gap between two dates  $dt = T/n$ , the underlying price starting at  $S_0 = 100$ , a risk free rate  $r = 10\%$ , and  $\sigma$  and  $K$  standing for the volatility and the strike price. (**Note:** We count in the starting point  $S_0$  as one observation, so that there are  $n + 1$  observation points to be averaged.)

In order to implement the algorithm efficiently, we should choose an appropriate grid to start with. Let us consider Benhamou's interpolation method, since the only

Table 4.1: Prices of Asian options with different choice of grid width

$2^m$	$9n\sigma\sqrt{dt}$	CPU time (sec.)	$2n\sigma\sqrt{dt}$	CPU time (sec.)
10	22.776536941	0.75	22.777183089	0.77
11	22.777194560	2.46	22.777176650	2.55
12	22.777184768	8.14	22.777175350	9.54
13	22.777177372	28.88	22.777174997	36.63
14	22.777175472	112.49	22.777174911	138.58
15	22.777175025	438.01	22.777174889	553.87

two parameters we can choose are the grid width  $w$  and the number of grid points  $N$ . His choice of the grid width is  $9n\sigma\sqrt{dt}$ . However, it turns out to be too large so that the grid is sparse and more grid points are needed to obtain the satisfactory accuracy. One way to find a finer grid is that given a very large number of grid points, say  $2^{15}$  or  $2^{16}$ , we could expand the grid width gradually until the answer stops changing. Then we can say this grid width is fine. In the case that  $\sigma = 0.1$  and  $K = 80$ , we find that  $2n\sigma\sqrt{dt}$  is large enough to be the width, and the answer stops changing at 22.77717488 (using the first 10 digits). We compare the results of Asian options with different choices of width in Table 4.1.

Obviously, we find that we need fours times the number of grid points to get the same accuracy with width  $9n\sigma\sqrt{dt}$  as with  $2n\sigma\sqrt{dt}$ , since the width is 4.5 times larger. For example, we obtain the first 7 digits using  $2^{11}$  points with width  $2n\sigma\sqrt{dt}$  while we need  $2^{13}$  points with width  $9n\sigma\sqrt{dt}$ .

In addition, we find in Table 4.1 that the CPU time almost quadrupled when the number of grid points doubled. This is due to the computation cost of the convolution in Matlab, since the convolution contains two forward Fourier transforms and one inverse transform. The performance of the algorithm can be improved by

Table 4.2: The computation time of using characteristic function and using convolution

$2^m$	Convolution	CPU time (sec.)	Char. Function	CPU time (sec.)
10	22.777183089	0.77	22.777183089	0.39
11	22.777176650	2.55	22.777176650	0.75
12	22.777175350	9.54	22.777175350	1.23
13	22.777174997	36.63	22.777174997	2.40
14	22.777174911	138.58	22.777174911	4.81
15	22.777174889	553.87	22.777174889	10.66

directly using the characteristic functions. Instead of doing all the interpolation and convolution in the real space, we switch from the real space to the Fourier space. This implies that the convolution of two density functions is replaced by the multiplication of two characteristic functions in the Fourier space. The computing time can be greatly reduced by this change. The NFFT method will benefit more from this change because we always need the Fourier coefficients to do the NFFT whether or not we have the density function. We follow the previous example and use the grid width as  $2n\sigma\sqrt{dt}$  to demonstrate. The computation time of using characteristic function and using convolution are compared in Table 4.2.

We get exactly the same answers in these two method, however, the computation time only doubled when the number of grid points doubled by using the characteristic functions directly. The performance is improved dramatically when the number of grid points is large.

While carefully choosing the width of the grid, and computing the convolutions in the Fourier space, can improve performance dramatically, the most significant improvement in performance arises from using the NFFT method in combination

with Gaussian quadrature or Romberg integration. To investigate the efficiency of the NFFT algorithm, we need the ‘exact’ value which all these algorithms converge to. We obtain this by setting all the parameters in our algorithm large enough so that the final answer does not change any more. There are more parameters we can set besides the width  $w$  and the number of grid points  $N$ . They are the degree of the NFFT polynomial  $m$ , the oversampling factor  $s$ , the number of Gaussian points and the number of Romberg points. We find that if we choose grid width  $w = 2n\sigma\sqrt{dt}$ ,  $m = 30$ ,  $s = 2$ , and  $NGaussian = 50$  or  $NRomberg = N$ , these parameters are large enough to get the desired unchanged value, and this exact value turns out to be 22.777174882763 in this case. Actually, all the methods converge to this value as seen above. Then the accuracy can be represented by taking  $\log_{10}$  of the absolute error:

$$\log_{10} |(P - P_{exact})/P_{exact}|. \quad (4.1)$$

By this formula, we compare the accuracy of the NFFT method with Gaussian quadrature, the NFFT method with Romberg integral, the cubic interpolation method with trapezoid rule and the cubic interpolation method with Gaussian quadrature. We use the same parameters in these different algorithm as specified above. The comparison is given in Table 4.3 and Figure 4.1.

We observe that the cubic interpolation method with trapezoid rule offers the slowest rate of convergence, because of the low error order of the trapezoid rule. The interpolation with Gaussian quadrature converges faster than it with trapezoid rule, since Gaussian quadrature offers enough accuracy to match the order of accuracy of the cubic interpolation. It is obvious that the NFFT method with Gaussian quadrature or Romberg integration converges much more quickly than the interpo-

Table 4.3: The comparison of different algorithms

$2^m$	Interp (Trapezoid)	CPU time (sec.)	Interp (Gaussian)	CPU time (sec.)
6	26.875881200769729	0.09	26.873694063988005	0.10
7	22.825907813457029	0.10	22.825443458704967	0.12
8	22.776665657688902	0.15	22.776549814345938	0.15
9	22.777204555868696	0.22	22.777175592683204	0.23
10	22.777183089437347	0.39	22.777175848393469	0.49
11	22.777176650380930	0.75	22.777174840288946	0.77
12	22.777175349834323	1.23	22.777174897290497	1.38
13	22.777174996880014	2.40	22.777174883738827	2.55
14	22.777174911089951	4.81	22.777174882807628	5.06
15	22.777174889835759	10.66	22.777174882764932	11.28
$2^m$	NFFT (Gaussian)	CPU time (sec.)	NFFT (Romberg)	CPU time (sec.)
6	25.423538733516917	0.09	25.423719613205169	0.15
7	22.777404185288173	0.18	22.777403582735875	0.17
8	22.777174882762822	0.33	22.777174883342173	0.35
9	22.777174882762992	0.63	22.777174882762839	0.69
10	22.777174882762949	1.23	22.777174882762925	1.33
11	22.777174882762957	2.56	22.777174882762985	2.63
12	22.777174882762939	4.99	22.777174882762985	5.14
13	22.777174882762885	10.29	22.777174882762900	10.33
14	22.777174882762942	20.09	22.777174882762893	20.94
15	22.777174882762928	41.22	22.777174882762846	42.53

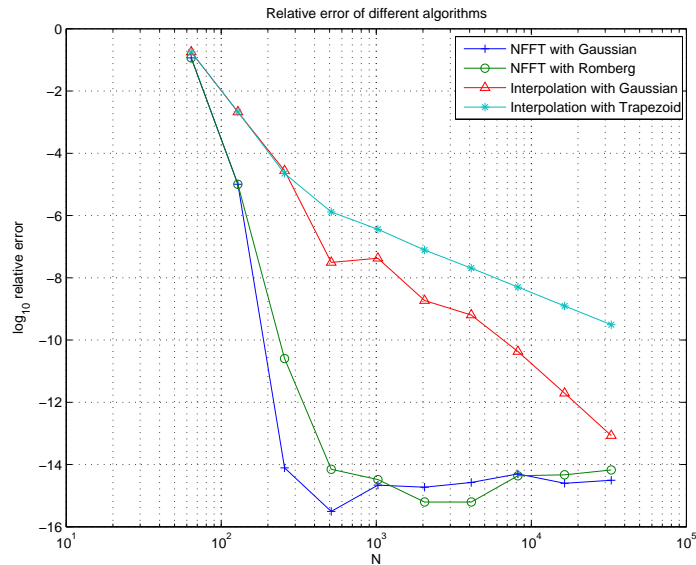


Figure 4.1: Relative error of different algorithms

lation method even with Gaussian quadrature. This is because of the exponential convergence rate of the NFFT method. This also means that we could use fewer grid points to get the same accuracy or we could use the same grid points to get more accurate digits using the NFFT method. In this case, we only need  $2^8 = 256$  points to get first 14 accurate digits which only takes 0.33 seconds, while using the interpolation, we need  $2^{15}$  to get first 10 digits and it costs about 11 seconds. Even if we use more accurate Gaussian quadrature with the interpolation,  $2^{15}$  points offers us first 13 digits. Besides, we also observe that the rate of convergence of Gaussian quadrature and Romberg integral are almost the same. We say we prefer Gaussian quadrature to Romberg integral since it is faster in computation and converges a bit faster in our case.

Therefore, we use these sets of parameter as our default settings in the NFFT method to price Asian options under the log-normal model and compare the NFFT method with other methods. The results are presented in Table 4.4, where CC stands for Carverhill and Clewlow's method without recentering the density, Interp stands for the interpolation with Gaussian quadrature using  $2^{12}$  points and NFFT stands for the NFFT method with Gaussian quadrature using  $2^8$  points.

We find that both the NFFT algorithm and the interpolation algorithm work well for the low volatility and high volatility, and for out-of-the-money and in-the-money. These two methods offer similar results which are closer to the Monte Carlo result than the CC one, especially the volatility is high. We get excessive accuracy in these two methods which means we can use fewer grid points in practice to get desired accuracy.

## 4.2 Continuous Case Approximation

Many authors have considered the pricing of continuously-averaged Asian options. Hull and White [42], Forsyth et al. [30] and Hsu and Lyuu [41] use discrete case Asian options to approximate the continuous case. In addition, some others provide semi-analytical formula for continuous Asian options directly (see [74, 69, 32, 19]).

We extend our algorithm to approximate the continuous time Asian options by letting the number of observation dates  $n$  go to infinity. However, we can not simply set  $n$  a large number and use the same parameters as in the previous section, since when  $n$  increases, the density of the log-return peaks, and more grid points are needed to resolve it. Fortunately, we only use the characteristic function as input

Table 4.4: The comparison of the different methods for the Asian option

$\sigma$	K	MC	CC	Interp	NFFT
10%	80	22.78	22.78	22.77717490	22.77717488
	90	13.73	13.73	13.73377727	13.73377726
	100	5.24	5.25	5.248992711	5.248992708
	110	0.72	0.72	0.723832356	0.723832356
	120	0.03	0.02	0.026409201	0.026409201
30%	80	23.07	23.09	23.09143781	23.09143780
	90	15.22	15.29	15.22076100	15.22076100
	100	9.01	9.08	9.027188773	9.027188768
	110	4.83	4.86	4.834907139	4.834907137
	120	2.35	2.40	2.368285453	2.368285452
50%	80	24.83	25.01	24.82425812	24.82425813
	90	18.32	18.50	18.33167403	18.33167403
	100	13.18	13.47	13.15804557	13.15804557
	110	9.23	9.45	9.234513354	9.234513356
	120	6.36	6.68	6.371953631	6.371953632

in the algorithm. It becomes flatter when  $n$  increases, which enables us to address the continuous case. The most important thing here is still to choose an appropriate grid width and number of grid points such that our results stop changing when  $n$  is a very large number. Since the initial density function peaks as  $n$  increases, we expect that the grid width should be smaller as  $n$  increases to fit the support of the initial density. We find that  $9\sigma\sqrt{dt}$  is suitable to cover the support of the initial density. However, as  $n$  increases, the evolution of the density functions tends to require a wider grid. After careful testing, we find that the rate at which the grid width increases is roughly proportional to  $\sqrt{n}$ . These two phenomena just compensate the effect of the change of  $n$ , which implies that the previous width  $w = 2n\sigma\sqrt{dt}$  is not good in this case since it increases as  $n$  increases. In the continuous case, we finally

Table 4.5: The comparison of approximations to continuous Asian options

$n$	Hull-White	Forsyth	Hsu-Lyuu	NFFT
case 1: $S_0 = 100, K = 100, r = 0.1, \sigma = 0.1, T = 0.25$				
50	1.8486	1.8478	1.8714720	1.846680705
100	1.8501	1.8492	1.9095930	1.849114102
200	1.8508	1.8503	1.8891953	1.850347590
400	1.8512	1.8509	1.8703678	1.850968598
1000	-	-	-	1.851342578
$\infty$	1.8516	1.8514	1.8515402	1.851467468
case 2: $S_0 = 100, K = 100, r = 0.1, \sigma = 0.5, T = 0.5$				
50	28.3899	28.3573	28.3893142	28.36950709
100	28.3972	28.3842	28.3973455	28.38695401
200	28.4011	28.3952	28.4013633	28.39595728
400	28.4031	28.4003	28.4032833	28.40052964
1000	-	-	-	28.40329559
$\infty$	28.4051	28.4054	28.4052033	28.40422118

choose the grid with as  $w = 9\sigma\sqrt{T}$  and number of grid points as  $N = 2^{10}$ . Other parameters are the same as the discrete case:  $m = 30, s = 2$  and  $NGaussian = 50$ . We let  $n = 2000$  as our continuous case approximation. This set of parameters works well in this case and also in cases when  $n$  is small. We compare our results with other discrete case approximation in Table 4.5. The exact value in case 1 is  $1.8515 \pm 0.0001$  and that in case 2 is  $28.40525 \pm 0.00015$  (see [30]). We compare our results with other continuous case pricing methods in Table 4.6. We take Zhang [74] as the exact value of continuous Asian option. The computation time in our algorithm for the continuous case is about 55 seconds. We find that our algorithm produces almost the same results as various pricing methods for the continuous Asian options, which demonstrates the correctness of our algorithm.

Table 4.6: The comparison of different methods for continuous Asian options with  $S_0 = 100$ ,  $r = 0.09$  and  $T = 1$

$K$	$\sigma$	Exact	Vecer	Fusai	Chen-Lyuu	NFFT
95		8.8088392	8.8088241	8.80885	8.8088389	8.808870993
100	0.05	4.3082350	4.3080602	4.30824	4.3082311	4.308226113
105		0.9583841	0.9583277	0.95839	0.9583309	0.958276284
95		8.9118509	8.9118054	8.91185	8.9118360	8.911816396
100	0.1	4.9151167	4.9150253	4.91512	4.9150753	4.914953892
105		2.0700634	2.0700251	2.07007	2.0699297	2.069832589
95		9.9956567	9.9956323	-	9.9953622	9.995310751
100	0.2	6.7773481	6.7773279	-	6.7769994	6.776896339
105		4.2965626	4.2964614	-	4.2959409	4.295984820
95		13.5107083	13.5107373	-	13.5078924	13.50976191
100	0.4	10.9237708	10.9238049	-	10.9208908	10.92278456
105		8.7299362	8.7299758	-	8.7268042	8.728960972

### 4.3 Comparison among the Lévy Models

From our algorithm, we only have the characteristic function and the recentering parameter  $(m_i)_{i=1\dots n}$  as our inputs. Therefore, to apply this algorithm to other Lévy process, we only need to change the characteristic function and compute the mean of the associated log returns. Formulae for the characteristic functions of different Lévy processes are provided in Section 1.2.3. In order to compare the price of an Asian option under different Lévy models with the one under the log-normal model, we need the parameters of the underlying processes calibrated from the same data set. For this purpose, we quote the calibrated parameters from [62] as follows:

The calibrated volatility parameter for the log-normal model is  $\sigma = 0.17801$ .

The calibrated parameters for the Merton's jump diffusion model are  $\sigma = 0.126349$ ,  $\alpha = -0.390078$ ,  $\lambda = 0.174814$  and  $\delta = 0.338796$ .

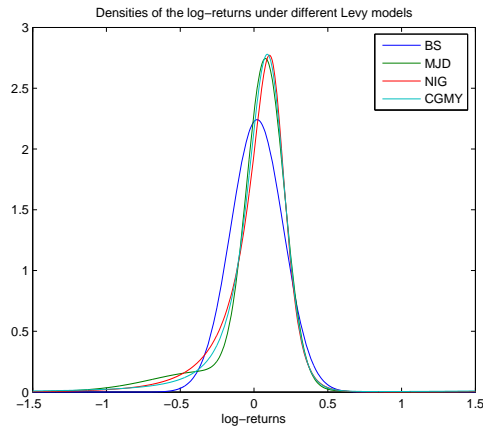


Figure 4.2: Densities of the log-returns in 1 year

The calibrated parameters for the NIG model are  $\alpha = 6.1882$ ,  $\beta = -3.8941$  and  $\delta = 0.1622$ .

The calibrated parameters for the CGMY model are  $C = 0.0244$ ,  $G = 0.0765$ ,  $M = 7.5515$  and  $Y = 1.2945$ .

Though they are calibrated from the market data of S&P 500 European options, which are not the best for Asian options, we just want to use them to implement our algorithm for these Lévy processes. The densities of the log-returns modelled by these Lévy processes in the risk-neutral world are plotted in Figure 4.2. We observe that the densities of Merton's jump diffusion, NIG and CGMY are similar to each other. They show negative skewness and fat-tail phenomenon and are quite different from the log-normal one. To be specific, the skewness and kurtosis can be calculated respectively as -2.16016 and 7.46374 for the Merton's model, -2.13745 and 9.93736 for the NIG model, and -19.813 and 986.936 for the CGMY model.

We compute a one-year Asian option with initial value  $S_0 = 100$ , the risk free rate

Table 4.7: The comparison of Asian option prices under different Lévy models

$n$	$K$	LN	MJD	NIG	CGMY
12	90	11.90491575	12.71066914	12.62281214	13.33610440
12	100	4.881961617	5.011289912	5.060591604	5.604338195
12	110	1.363037953	1.051632904	1.013550654	1.531915855
50	90	11.93293834	12.74094241	12.66128680	13.36937104
50	100	4.937202879	5.052459656	5.103737740	5.646839831
50	110	1.402515536	1.079596752	1.037738449	1.560106138
250	90	11.94056316	12.74918192	12.67563282	13.37799740
250	100	4.952156881	5.063822925	5.118441942	5.658149424
250	110	1.413367031	1.087405588	1.046823143	1.567639555

$r = 0.0367$ , strike price  $K$  and  $n$  observation dates. For the log-normal model, we just use the default parameters as in the previous section: grid width  $w = 2n\sigma\sqrt{dt}$ ,  $m = 30$ ,  $s = 2$ ,  $NGaussian = 50$  and  $2^8$  grid points.

For other Lévy processes, we should choose the parameters carefully to find their converged values. Finally, we use  $2^{10}$  points for Merton's jump diffusion model,  $2^{14}$  points for NIG model and  $2^{12}$  for CGMY model. The comparison of the prices of Asian options under different Lévy models with different observations is given in Table 4.7.

From Table 4.7, we note that the prices of Asian options tend to increase when the number of observation dates increase. The prices under other Lévy models are a bit higher than the log-normal one, since their densities have fat-tails. The reason why we need much more grid points for NIG and CGMY model is that their transition densities peak dramatically when the observation dates increase. So more points are needed to resolve the density correctly. The comparison of the density of  $A_n$  and the average  $A$  can be found in Figure 4.3.

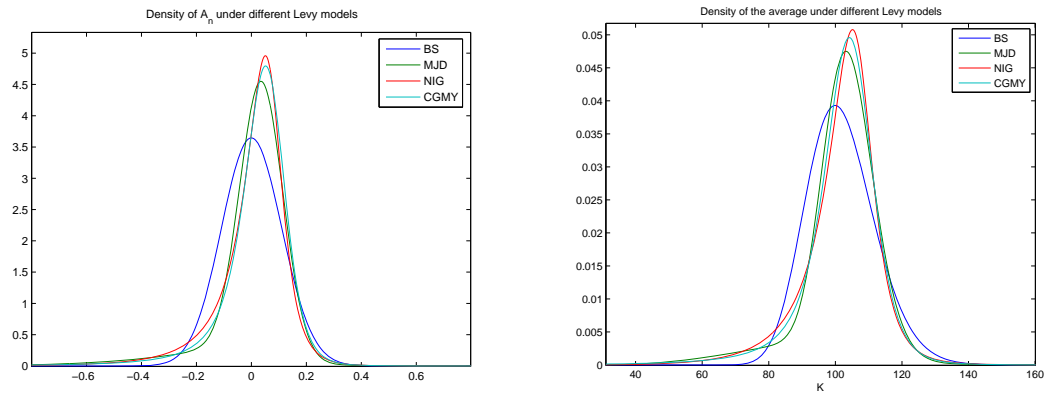


Figure 4.3: Left: Density of  $A_n$  under different Lévy models. Right: Density of the average under different Lévy models.

From the discussion above, we conclude that the NFFT algorithm offers a high rate of convergence compared with the interpolation method in pricing Asian options. Hence, we can use fewer grid points to obtain the same accuracy, which speeds up the computation dramatically. Besides, our method can be easily extended to price the continuous Asian options and Asian options under other exponential Lévy models. The option prices are a bit higher under other Lévy models than the log-normal one.

## Chapter 5

# Option Pricing Based on the Semi-Lagrangian Method

In this chapter, we will apply the NFFT to price other kinds of options by using the semi-Lagrangian method. In the first section, we will provide a brief introduction to the semi-Lagrangian scheme for differential equations. Based on this scheme, we are able to evaluate European and American options under a general class of diffusion processes which includes popular mean-reverting processes. We will present an algorithm for pricing European options through transition densities and take the simple Ornstein-Uhlenbeck (OU) process and Cox-Ingersoll-Ross (CIR) process as examples in Section 5.2. In Section 5.3, a direct algorithm for pricing options is discussed, which allows us to price European and American calls and puts under Lévy processes or Lévy-driven mean-reverting processes.

### 5.1 The Semi-Lagrangian Method

The semi-Lagrangian method is a numerical technique originally introduced to solve advection equations in [23]. Unlike the Lagrangian method in which the equally spaced grid will finally evolve into an unequally spaced grid, the semi-Lagrangian method allows us to compute on a equally spaced grid. At each time step, we choose different points so that they exactly arrive at the equally spaces grid in the end under the action of the advection. A good review of the semi-Lagrangian method can be

found in [64], and one could also refer to [13, 71] for details about the applications of this method. Here we just briefly introduce this method.

Consider the following advection equation

$$\frac{\partial u}{\partial t} + a \cdot \nabla u = 0 \quad (5.1)$$

with initial condition  $u(x, 0) = u_0$  and  $a = a(x, t)$ .

We define a function  $X(x, t_0; t), t_0 \in [0, T]$  to be the solution to the following ordinary differential equation (ODE):

$$\frac{d}{dt}X(x, t_0; t) = a(X(x, t_0; t), t) \quad (5.2)$$

with initial condition  $X(x, t_0; t_0) = x$ . With sufficient smoothness of  $u$  and  $a$ , the chain rule leads to

$$\begin{aligned} \frac{d}{dt}u(X(x, t_0; t), t) &= u_t(X(x, t_0; t), t) + \frac{d}{dt}X(x, t_0; t) \cdot \nabla u(X(x, t_0; t), t) \\ &= [u_t + a \cdot \nabla u](X(x, t_0; t), t) \\ &= 0. \end{aligned}$$

Thus, the solution to (5.1) satisfies

$$u(X(x, t_0; t), t) = \text{constant}, \quad (5.3)$$

and, by the initial conditions, we have

$$u(x, t) = u_0(X(x, t; 0)), \quad (5.4)$$

We discretize (5.4) in time  $[0, T]$  with  $t^n = n\Delta t, n = 1, \dots, N$  and  $\Delta t = T/N$ . We denote  $u^n(x) = u(x, t^n)$ . The semi-Lagrangian scheme expresses  $u^{n+1}$  at the

equally spaced grid points in terms of  $u^n$  at points of a grid that within a single time step will be transported by the flow  $X(x, t; t^n)$  onto the original grid. The solution is evolved step-by-step via:

$$u^{n+1}(x) = u^n(X(x, t^{n+1}; t^n)), \quad n = 0, \dots, N - 1. \quad (5.5)$$

This guarantees that, overall, the grid does not change in time. Given the solution to (5.2), we can apply the Fourier transform to both sides of (5.5) to work in the Fourier space, and then at each time step  $n$ , the NFFT can be used to evaluate the solution  $u^n$  at an unequally spaced grid so that  $u^{n+1}$  arrives at the equally spaced grid. After that, we apply the inverse transform to go back to the Fourier space again and continue doing these in the next step.

## 5.2 Pricing Options through Transition Densities

In Chapter 3, we proposed a recursive algorithm for Asian options by computing the evolution of the probability density of the sum of two random variables using the NFFT. For any diffusion process

$$dX_t = \mu(X_t)dt + \sigma(X_t)dW_t, \quad (5.6)$$

given the initial density  $p_0(x)$ , the following partial differential equation (PDE) describes the evolution of the probability density  $p(x, t)$  for  $X_t$ :

$$\frac{\partial p(x, t)}{\partial t} = -\frac{\partial}{\partial x}[\mu(x, t)p(x, t)] + \frac{1}{2}\frac{\partial^2}{\partial x^2}[\sigma^2(x, t)p(x, t)]. \quad (5.7)$$

The equation is called Fokker-Planck equation or Kolmogorov forward equation (see [33] for details).

In terms of option pricing, we take the log-transform of the asset price  $S_t$  and denote  $x_t = \ln(S_t/S_0)$ . If the return series  $x_t$  follows the SDE

$$dx_t = \mu(x_t)dt + \sigma dW_t, \quad (5.8)$$

with initial condition  $x_0 = 0$ , then the associated Fokker-Planck equation is given by

$$p_t + (\mu p)_x - \frac{\sigma^2}{2} p_{xx} = 0. \quad (5.9)$$

We solve this equation using the semi-Lagrangian scheme and implement the algorithm via the NFFT. After obtaining the probability density  $p(x, T)$  at maturity  $T$ , finding the price of an European option is quite straightforward; by the risk-neutral pricing formula,

$$\begin{aligned} P &= e^{-rT} \mathbb{E}^{\mathbb{Q}}[(S_T - K)_+] \\ &= e^{-rT} \int_{\ln(K/S_0)}^{\infty} (S_0 e^{xT} - K) p(x, T) dx. \end{aligned} \quad (5.10)$$

This can be easily computed by careful numerical integration, for example Gaussian quadrature.

To solve (5.9), we apply the weak Lagrange-Galerkin method, a version of the semi-Lagrangian approach. The weak Lagrange-Galerkin method is a finite element method for PDEs, and the details can be found in [11, 36, 71]. We let  $\psi(x, t)$  be a test function and integrate (5.9) in space and time against this test function. Denote  $\langle f, g \rangle = \int_{\mathbb{R}} f \cdot \bar{g} dx$ , the inner product in  $\mathbb{R}$ . Then we have:

$$\int_{t^m}^{t^{m+1}} \langle p_t + (\mu p)_x - \frac{\sigma^2}{2} p_{xx}, \psi \rangle dt = 0. \quad (5.11)$$

Since  $(\psi p)_t = \psi_t p + \psi p_t$ , after integrating by parts, we obtain the following

$$\int_{t^m}^{t^{m+1}} \langle (\psi p)_t + \frac{\sigma^2}{2} p_x \psi_x, 1 \rangle dt = \int_{t^m}^{t^{m+1}} \langle p, \psi_t + \mu \psi_x \rangle dt. \quad (5.12)$$

Setting  $\psi(x, t) = \phi(X(x, t)) = e^{-ikX}$ , we have

$$\psi_t + \mu\psi_x = \phi'(X)(X_t + \mu X_x). \quad (5.13)$$

If we choose  $X(x, t)$  such that  $X_t + \mu X_x = 0$  and  $X(x, t^{m+1}) = x$ , then

$$\langle \psi^{m+1}, p^{m+1} \rangle - \langle \psi^m, p^m \rangle \approx -\frac{\sigma^2}{2} \Delta t \langle \psi_x^{m+1}, p_x^{m+1} \rangle. \quad (5.14)$$

Since  $\psi^{m+1} = \phi(X^{m+1}) = \phi(x)$ , we have

$$\langle \phi(x), p^{m+1} \rangle - \langle \phi(X^m), p^m \rangle \approx -\frac{\sigma^2}{2} \Delta t \langle \phi'(x), p_x^{m+1} \rangle. \quad (5.15)$$

As  $\phi(x) = e^{-ikx}$ ,  $\langle \phi(x), p^{m+1} \rangle$  is just the Fourier coefficients of  $p^{m+1}$ , denoted as  $\widehat{p_x^{m+1}}(k)$ . By the properties of the Fourier transform,  $\langle \phi'(x), p_x^{m+1} \rangle = k^2 \widehat{p_x^{m+1}}(k)$ . By a change of variable, we have

$$\begin{aligned} \langle \phi(X^m), p^m \rangle &= \int_{\mathbb{R}} e^{ikX(x, t^m)} p(x, t^m) dx \\ &= \int_{\mathbb{R}} e^{ikX(x, t^m)} \cdot \frac{1}{X'(x, t^m)} p(x, t^m) dX \\ &= \int_{\mathbb{R}} e^{ikX} p^m(X) dX, \end{aligned} \quad (5.16)$$

where  $p^m(X)$  is exactly the probability density of the random variable  $X$  at time  $t^m$ . Then (5.16) is the Fourier coefficients of density  $p^m(X)$ , denoted as  $\widehat{p_X^m}(k)$ . Therefore, (5.15) can be written as

$$\widehat{p_x^{m+1}}(k) - \widehat{p_X^m}(k) \approx -\frac{\sigma^2}{2} \Delta t k^2 \widehat{p_x^{m+1}}(k), \quad (5.17)$$

which yields

$$\left(1 + \frac{\sigma^2}{2} \Delta t k^2\right) \widehat{p_x^{m+1}}(k) \approx \widehat{p_X^m}(k). \quad (5.18)$$

This can be implemented via the NFFT, which is the same as we did in the semi-Lagrangian scheme.

Given the Fourier coefficients  $\widehat{p}_x^m(k)$ , we apply the NFFT to evaluate  $p^m(x)$  at an unevenly-spaced grid so that  $p^m(X)$  is on an evenly-spaced grid. Then we apply the IFFT to find the Fourier coefficients  $\widehat{p}_X^m(k)$  and compute  $\widehat{p}_x^{m+1}(k)$  by (5.18). After obtaining  $\widehat{p}_x^M(k)$  with  $t^M = T$ , we apply the NFFT again to evaluate  $p(x, T)$  at Gaussian grid points so that we are able to compute the price of European options by (5.10) using Gaussian quadrature. The algorithm is summarized in Algorithm 3 and its computational complexity is  $\mathcal{O}(2MN \log N + MI)$ , where  $I$  is the number of unevenly-spaced points.

---

**Algorithm 3** Option pricing through transition densities

---

1. Choose a fine grid  $[-w, w]$  with  $N$  points.
2. Compute  $\widehat{p}_x^1(k)$ .
3. Loop  $m = 1$  to  $M$ . **Input:**  $\widehat{p}_x^m(k)$ .
  - Deduce the unevenly-spaced grid by taking  $X^{-1}(x, t^m)$ .
  - Evaluate  $p^m(x)$  on the unevenly-spaced grid via the NFFT.
  - Evaluate  $p^m(X)$  on the evenly-spaced grid.
  - Compute  $\widehat{p}_X^m(k)$  by the IFFT.
  - By (5.18),  $\widehat{p}_x^{m+1}(k) \approx \widehat{p}_X^m(k)/(1 + \frac{\sigma^2}{2} \Delta t k^2)$ .

End Loop. **Output:**  $\widehat{p}_x^{m+1}(k)$ .

4. Compute  $P$  by Gaussian quadrature.
- 

$$\begin{array}{ccccc}
 \text{Fourier space:} & \widehat{p}_x^m(k) & & \widehat{p}_X^m(k) & \longrightarrow & \widehat{p}_x^{m+1}(k) \\
 & \text{NFFT} \downarrow & & \uparrow \text{IFFT} & & \\
 \text{Real space:} & p^m(x)(\text{uneven}) & \xrightarrow{X=X(x, t^m)} & p^m(X)(\text{even}) & & 
 \end{array}$$

Therefore, given any diffusion processes (5.8) with drift  $\mu(x)$  or any processes which can be transformed into this type, as long as we can find  $X(x, t)$  such that  $X_t + \mu X_x = 0$  and  $X(x, t^{m+1}) = x$ , the price of European options can be calculated by our algorithm. We will take the OU process and the CIR process as examples in the following sections.

### 5.2.1 European Options under the OU Processes

We assume that the return series satisfies the simple OU process:

$$dx_t = (a - bx_t)dt + \sigma dW_t, \quad (5.19)$$

with initial condition  $x_0 = 0$ . In this case,  $\mu(x) = a - bx$ . We start from such OU process because the density function of  $x_t$  can be solved analytically, which yields a closed form solution for the price of European options. Thus, it is easy to check our algorithm. In this case,  $x_t$  turns out to be normally-distributed with mean  $\zeta(t)$  and variance  $\eta(t)$ :

$$\zeta(t) = x_0 e^{-bt} + \frac{a}{b}(1 - e^{-bt}), \quad (5.20)$$

and

$$\eta(t) = (1 - e^{-2bt}) \frac{\sigma^2}{2b}. \quad (5.21)$$

The density of  $x_t$  is given by

$$p(x, t) = \sqrt{\frac{b}{\pi\sigma^2(1 - e^{-2bt})}} \exp\left(\frac{-b(x - x_0 e^{-bt} - \frac{a}{b}(1 - e^{-bt}))^2}{\sigma^2(1 - e^{-2bt})}\right). \quad (5.22)$$

With this density function, we can find a Black-Scholes formula-like solution to the price of European call options:

$$P = S_0 e^{-rT + \zeta + \frac{\eta^2}{2}} N(d1) - K e^{-rT} N(d2), \quad (5.23)$$

where

$$d1 = \frac{\ln(S_0/K) + \zeta + \eta^2}{\eta},$$

$$d2 = \frac{\ln(S_0/K) + \zeta}{\eta},$$

and  $\zeta = \zeta(T)$ ,  $\eta = \eta(T)$ .

To compute this price numerically by our algorithm, we only need to find  $X(x, t)$  such that  $X_t + (a - bx)X_x = 0$  and  $X(x, t^{m+1}) = x$ .

We define  $z(t; x)$  such that

$$\frac{dz}{dt} = a - bz, \quad (5.24)$$

and

$$z(t^{m+1}) = x. \quad (5.25)$$

The solution to (5.24) with (5.25) is given by

$$z = xe^{b(t^{m+1}-t)} - \frac{a}{b}(e^{b(t^{m+1}-t)} - 1). \quad (5.26)$$

Since

$$\frac{d}{dt}X(z(t), t) = X_z \cdot \frac{dz}{dt} + X_t = X_t + (a - bz)X_z = 0,$$

then

$$X(z(t), t) = \text{constant},$$

$$X(z(t^{m+1}), t^{m+1}) = X(x, t^{m+1}) = x. \quad (5.27)$$

By solving (5.26), we have

$$x = ze^{b(t-t^{m+1})} + \frac{a}{b}(1 - e^{b(t-t^{m+1})}). \quad (5.28)$$

Table 5.1: Prices of European call options under the OU process

$M \setminus N$	$2^8$	$2^9$	$2^{10}$
1000	24.82060765	24.82057960	24.82058089
2000	24.81399431	24.81395183	24.81395115
3000	24.81178837	24.81174256	24.81174053
5000	24.81002230	24.80997502	24.80997199
10000	24.80869639	24.80864915	24.80864554

Therefore,

$$X(z, t) = ze^{b(t-t^{m+1})} + \frac{a}{b}(1 - e^{b(t-t^{m+1})}), \quad (5.29)$$

$$X(x, t) = xe^{b(t-t^{m+1})} + \frac{a}{b}(1 - e^{b(t-t^{m+1})}). \quad (5.30)$$

Since  $x_0 = 0$ , the initial density  $p_0(x)$  is just a Dirac delta function. We can find  $\widehat{p}_x^1(k)$  by

$$\begin{aligned} \widehat{p}_x^1(k) &= \frac{e^{ikX(0)}}{1 + \frac{\sigma^2}{2}\Delta tk^2} \\ &= \frac{e^{ik\frac{a}{b}(1-e^{-b\Delta t})}}{1 + \frac{\sigma^2}{2}\Delta tk^2}. \end{aligned} \quad (5.31)$$

From this point, we follow our algorithm to price European call options. Here is an example:  $a = 0.2$ ,  $b = 0.5$ ,  $\sigma = 0.1$ ,  $r = 0.1$ ,  $T = 1$ ,  $S_0 = 100$  and  $K = 90$ . The exact solution is 24.80732115 by (5.23). We choose grid width  $w = 1.2$ , the degree of the NFFT polynomial  $m = 15$  and the number of Gaussian points  $NGaussian = 50$ . Prices of European calls are given in Table 5.1.

The exact solution 24.80732115 represents the price of the option in the continuous case. From Table 5.1, we find that as the number of time steps increases, the results converge to this exact value. However, the increase of the grid points does not

improve the accuracy dramatically. We say that we do not need many grid points, but need more time steps to get more correct digits. In this example, if we use 5000 time steps and  $2^8$  grid points, we obtain 4 digits, which takes 23 seconds to compute.

### 5.2.2 European Options under the CIR Processes

We assume that the return series satisfies the CIR process:

$$dx_t = (a - bx_t)dt + \sigma\sqrt{x_t}dW_t, \quad (5.32)$$

with initial condition  $x_0 = 0$ . Since the CIR process is not the type of process (5.8), we first apply a change of variable and transform it into this form.

Let  $y_t = \sqrt{x_t}$  and by Itô's lemma, we have

$$\begin{aligned} dy_t &= \left[ \left( \frac{a}{2} - \frac{\sigma^2}{8} \right) \frac{1}{y_t} - \frac{b}{2}y_t \right] dt + \frac{\sigma}{2}dW_t \\ &= \left( \frac{\alpha}{y_t} - \beta y_t \right) dt + \gamma dW_t. \end{aligned} \quad (5.33)$$

where  $\alpha = \frac{a}{2} - \frac{\sigma^2}{8}$ ,  $\beta = \frac{b}{2}$  and  $\gamma = \frac{\sigma}{2}$ . So we can apply our algorithm to find the density of  $y_t$  and in this case,  $\mu(y) = \frac{\alpha}{y} - \beta y$ .

We only need to find  $X(y, t)$  such that  $X_t + (\frac{\alpha}{y} - \beta y)X_y = 0$  and  $X(y, t^{m+1}) = y, y > 0$ . We define  $z(t; y)$  such that

$$\frac{dz}{dt} = \frac{\alpha}{z} - \beta z, \quad (5.34)$$

and

$$z(t^{m+1}) = y. \quad (5.35)$$

The solution to (5.34) with (5.35) is given by

$$z^2 = \frac{\alpha}{\beta} - \left( \frac{\alpha}{\beta} - y^2 \right) e^{2\beta(t^{m+1}-t)}. \quad (5.36)$$

As  $y > 0$ ,  $z(t^{m+1}) = y > 0$ ,  $z > 0$ , So

$$z = \sqrt{\frac{\alpha}{\beta} - \left(\frac{\alpha}{\beta} - y^2\right)e^{2\beta(t^{m+1}-t)}}. \quad (5.37)$$

Since

$$\frac{d}{dt}X(z(t), t) = X_z \cdot \frac{dz}{dt} + X_t = X_t + (a - bz)X_z = 0,$$

then

$$X(z(t), t) = \text{constant},$$

$$X(z(t^{m+1}), t^{m+1}) = X(y, t^{m+1}) = y. \quad (5.38)$$

By solving (5.36), we have

$$y = \sqrt{\frac{\alpha}{\beta} - \left(\frac{\alpha}{\beta} - z^2\right)e^{2\beta(t-t^{m+1})}}. \quad (5.39)$$

Therefore,

$$X(z, t) = \sqrt{\frac{\alpha}{\beta} - \left(\frac{\alpha}{\beta} - z^2\right)e^{2\beta(t-t^{m+1})}}, \quad (5.40)$$

$$X(y, t) = \sqrt{\frac{\alpha}{\beta} - \left(\frac{\alpha}{\beta} - y^2\right)e^{2\beta(t-t^{m+1})}}. \quad (5.41)$$

In the CIR case, we can find

$$\widehat{p}_y^1(k) = \frac{e^{ik\sqrt{\frac{\alpha}{\beta}(1-e^{-2\beta\Delta t})}}}{1 + \frac{\gamma^2}{2}\Delta tk^2}. \quad (5.42)$$

Slightly different from the OU case, after we obtain  $\widehat{p}_y^M(k)$ , we compute the price of European call options by the following integration using Gaussian quadrature:

$$\begin{aligned} P &= e^{-rT} \mathbb{E}^{\mathbb{Q}}[(S_T - K)_+] \\ &= e^{-rT} \int_{\sqrt{(\ln(K/S_0))_+}}^{\infty} (S_0 e^{y^2} - K) p(y, T) dy. \end{aligned} \quad (5.43)$$

Table 5.2: Prices of European call options under the CIR process

$M \setminus N$	$2^{10}$	$2^{11}$	$2^{12}$	MC
500	24.51209388	24.51174193	24.53227399	24.54599822
1000	24.62596456	24.50501476	24.51709626	24.51686274
2000	24.66634641	24.49401584	24.49121972	24.49104656

Here is an example with the same parameters in the OU case:  $a = 0.2$ ,  $b = 0.5$ ,  $\sigma = 0.1$ ,  $r = 0.1$ ,  $T = 1$ ,  $S_0 = 100$  and  $K = 90$ . We choose grid width  $w = 0.65$ , the degree of the NFFT polynomial  $m = 15$  and number of Gaussian points  $NGaussian = 50$ . We compare the prices of European call options in our algorithm with the standard Monte Carlo simulation with 10000 paths. The standard error of the Monte Carlo is 0.029. The comparison is given in Table 5.2.

Compared with Monte Carlo method, we need  $2^{12}$  points to get the similar results. This is because the Fourier coefficients do not decay to zero very quickly. Although we use  $2^{12}$  points in our algorithm, it is still much faster than the Monte Carlo method. If the number of time steps is 1000, our algorithm only need 80 seconds while Monte Carlo takes 353 seconds. We also find that the European call options under the CIR process is a bit cheaper than those under the OU process with the same set of parameters.

### 5.3 Pricing Options Directly through PIDEs

An alternative way to price options based on the same idea of using the NFFT under the semi-Lagrangian scheme is to solve the pricing partial integro-differential equation (PIDE) directly. This algorithm is more accessible under the semi-Lagrangian

scheme, and provides us with flexibility to price European and American call and put options when the stochastic dynamics contains linear drift terms driven by general Lévy processes. Recently, many literature address the problem of pricing various type of options under Lévy processes [1, 2, 3, 4, 31, 40, 44, 52, 54], and the PIDE approach is one of the most popular methods among them (see [1, 26, 40, 44]). As we known, the option price in the Black-Scholes model is given by a second order parabolic PDE, while under a Lévy-driven process, it can be similarly described by a PIDE. We can price various type of options directly by solving such kind of PIDEs with different terminal or boundary conditions. In the following, I will show, in terms of the PIDEs, how the semi-Lagrangian scheme can be applied to price options under Lévy processes even with a mean-reverting drift term.

Generally speaking, when the asset price follows a diffusion process, for example, the geometric Brownian motion, the option price solves a PDE which can be derived based on the Feynman-Kac formula. Specifically, let  $x_t = \ln(S_t/S_0)$  be the log transform of asset price  $S_t$  and it follows the SDE in the risk-neutral measure  $\mathbb{Q}$ :

$$dx_t = \mu(x_t)dt + \sigma dW_t. \quad (5.44)$$

We also denote  $V(x, t) = \mathbb{E}^{\mathbb{Q}}[e^{-r(T-t)}h(X_T)|X_t = x]$  as the option price at  $t$ , where  $h(x)$  is the payoff function. Then  $V(x, t)$  solves the following parabolic PDE:

$$\frac{\partial V}{\partial t}(x, t) + \mu(x)\frac{\partial V}{\partial x}(x, t) + \frac{\sigma^2}{2}\frac{\partial^2 V}{\partial x^2}(x, t) = rV(x, t), \quad (5.45)$$

with terminal condition  $V(x, T) = h(x)$  for all  $x$ .

For a general jumps process, there is a generalized version of Feynman-Kac formula which enables us to derive a similar PIDE for the option price. We define a

jump process  $(X_s^{t,x})$  by

$$X_s^{t,x} = x + \int_t^s \gamma(u)du + \int_s^t \sigma(u)dW_u + \int_s^t \int_{|y|\geq 1} yJ_X(du dy) + \int_s^t \int_{|y|\leq 1} y\tilde{J}_X(du dy), \quad (5.46)$$

where  $W_t$  is a Brownian motion,  $J_X$  is the Poisson random measure with intensity  $\mu(dy dt) = \nu(dy)dt$  with Lévy measure  $\nu$ , and  $\tilde{J}_X$  is the compensated version of  $J_X$  with  $\tilde{J}_X(A) = J_X(A) - \int_A \nu(dy)dt$ . Then  $X_s^{t,x}$  is a jump process which starts at  $x$  at time  $t$  and has a drift term  $\gamma$ , a volatility term  $\sigma$  and a jump component described by Lévy measure  $\nu$ . If  $\gamma$  and  $\sigma$  are constant, then  $X_s^{t,x} = x + X_{s-t}$  where  $X$  is just a Lévy process with triplet  $(\gamma, \sigma^2, \nu)$  and (5.46) is the Lévy-Itô decomposition (1.4) in Section 1.2.2. The Feynman-Kac representation in this case can be summarized in the following proposition and details about this formula can be found in [22, 53, 57, 63].

**Proposition 5.3.1** (Feynman-Kac representation). *If  $X^{t,x}$  is a jump process given by (5.46), then the PIDE*

$$\begin{aligned} & \frac{\partial f}{\partial t}(t, x) + \gamma(t) \frac{\partial f}{\partial x}(t, x) + \frac{\sigma^2(t)}{2} \frac{\partial^2 f}{\partial x^2}(t, x) \\ & + \int [f(t, x+y) - f(t, x) - y1_{|y|<1} \frac{\partial f}{\partial x}(t, x)] \nu(dy) = 0, \end{aligned} \quad (5.47)$$

with terminal condition  $f(T, x) = h(x)$  for all  $x$ , has a unique solution  $f(t, x) = \mathbb{E}[h(X_T^{t,x})]$ .

Now consider that the log-transformed asset price  $x_t$  satisfies the following SDE in the risk-neutral measure  $\mathbb{Q}$ :

$$dx_t = \mu(x_t)dt + dL_t, \quad (5.48)$$

where  $\mu(x)$  is linear in  $x$  and  $L_t$  is a Lévy process with triplet  $(\gamma, \sigma^2, \nu)$ . Let

$$V(x, t) = \mathbb{E}^{\mathbb{Q}}[e^{-r(T-t)} h(X_T) | X_t = x]$$

be the option price at  $t$ , where  $h(x)$  is the payoff function. Based on the generalized version of Feynman-Kac representation (5.47), after a change of variable, we could similarly derive a corresponding PIDE for the option price  $V(x, t)$ :

$$\begin{aligned} & \frac{\partial V}{\partial t}(x, t) + [\mu(x) + \gamma] \frac{\partial V}{\partial x}(x, t) + \frac{\sigma^2}{2} \frac{\partial^2 V}{\partial x^2}(x, t) \\ & + \int [V(x + y, t) - V(x, t) - y1_{|y|<1} \frac{\partial V}{\partial x}(x, t)] \nu(dy) = rV(x, t), \end{aligned} \quad (5.49)$$

with terminal condition  $V(x, T) = h(x)$  for all  $x$ .

We denote  $v(x, t) = e^{rt}V(x, T - t)$ . Then  $v(x, 0) = V(x, T) = h(x)$  and the PIDE (5.49) is transformed into

$$\begin{aligned} \frac{\partial v}{\partial t}(x, t) &= e^{rt}[rV(x, T - t) - \frac{\partial V}{\partial t}(x, T - t)] \\ &= e^{rt}\left\{[\mu(x) + \gamma] \frac{\partial V}{\partial x}(x, T - t) + \frac{\sigma^2}{2} \frac{\partial^2 V}{\partial x^2}(x, T - t) \right. \\ &\quad \left. + \int [V(x + y, T - t) - V(x, T - t) - y1_{|y|<1} \frac{\partial V}{\partial x}(x, T - t)] \nu(dy)\right\} \\ &= [\mu(x) + \gamma] \frac{\partial v}{\partial x}(x, t) + \frac{\sigma^2}{2} \frac{\partial^2 v}{\partial x^2}(x, t) \\ &\quad + \int [v(x + y, t) - v(x, t) - y1_{|y|<1} \frac{\partial v}{\partial x}(x, t)] \nu(dy). \end{aligned} \quad (5.50)$$

When we introduce the infinitesimal generator  $\mathcal{L}$  defined in (1.8), (5.50) can be shortened as:

$$\frac{\partial v}{\partial t} = \mu(x) \frac{\partial v}{\partial x} + \mathcal{L}v, \quad (5.51)$$

with initial condition  $v(x, 0) = h(x)$ . The European option pricing problem under (5.48) with given payoff  $h(x)$  and  $x_0 = 0$  is reduced to evaluate  $v(x_0, T)$  by solving the PIDE (5.51).

Now we could apply the semi-Lagrangian method to (5.51) to eliminate the drift

term  $\mu(x)$ . We define a function  $X(x, t)$  such that

$$\frac{dX}{dt} = -\mu(X), \quad (5.52)$$

and  $X(x, t^{m+1}) = x$ . Then (5.51) leads to

$$\begin{aligned} \frac{dv}{dt} &= \frac{\partial v}{\partial X} \cdot \frac{dX}{dt} + \frac{\partial v}{\partial t} \\ &= -\mu(X) \frac{\partial v}{\partial X} + \frac{\partial v}{\partial t} \\ &= \mathcal{L}v. \end{aligned} \quad (5.53)$$

Discretizing the time interval  $[0, T]$  into  $M$  steps,  $m = 0, \dots, N - 1$ , gives us

$$v(x, t^{m+1}) - v(X(x, t^m), t^m) = \mathcal{L}v(x, t^{m+1}) \cdot \Delta t. \quad (5.54)$$

Denote  $v^m = v(x, t^m)$  and  $v_X^m = v(X(x, t^m), t^m)$ , we have

$$v^{m+1} - v_X^m = \mathcal{L}v^{m+1} \cdot \Delta t. \quad (5.55)$$

In the spirit of Jackson et al. [44], we should take the Fourier transform of both sides of (5.55) to get an iteration formula. We set the forward Fourier transform of a function  $f(x)$  as:

$$\hat{f}(\omega) = \mathcal{F}[f] = \int_{-\infty}^{\infty} f(x) e^{i\omega x} dx \quad (5.56)$$

By (1.9) for the infinitesimal generator, after taking this Fourier transform, (5.55) leads to

$$\widehat{v^{m+1}}(\omega) - \widehat{v_X^m} = \psi(-\omega) \widehat{v^{m+1}}(\omega) \cdot \Delta t, \quad (5.57)$$

where  $\psi(\omega)$  is the characteristic exponent of Lévy process  $L_t$ . We rearrange this

equation and obtain

$$\begin{aligned}
\widehat{v^{m+1}}(\omega) &= \frac{1}{1 - \psi(\omega)\Delta t} \widehat{v_X^{m+1}}(\omega) \\
&\approx e^{\psi(\omega)\Delta t} \widehat{v_X^{m+1}}(\omega) \\
&= \phi(\omega, \Delta t) \widehat{v_X^{m+1}}(\omega),
\end{aligned} \tag{5.58}$$

where  $\phi(\omega)$  is the characteristic function of Lévy process  $L_t$ .

Unlike the density function which decays to zero when we choose an appropriate grid, the payoff functions contain singularities in their Fourier transforms along the real line. So following [44], we introduce a shift factor  $\epsilon$  so that the iteration formula (5.58) is evaluated at  $\omega + i\epsilon$  instead of  $\omega$ . Then our modified iteration formula becomes:

$$\widehat{v_\epsilon^{m+1}}(\omega) = \phi_\epsilon(\omega, \Delta t) \widehat{v_{X,\epsilon}^{m+1}}(\omega). \tag{5.59}$$

where  $\phi_\epsilon(\omega, \Delta t) = \phi(\omega + i\epsilon, \Delta t)$  and

$$\widehat{v_\epsilon^m}(\omega) = \widehat{v^m}(\omega + i\epsilon) = \int_{-\infty}^{\infty} e^{i\omega x} [e^{-\epsilon x} v^m(x)] dx. \tag{5.60}$$

The inverse transform after shifting is given by

$$v^m(x) = \frac{e^{\epsilon x}}{2\pi} \int_{-\infty}^{\infty} \widehat{v_\epsilon^m}(\omega) e^{-i\omega x} d\omega. \tag{5.61}$$

This algorithm allows us to price European options under the jump process (5.48), which includes Lévy-driven or Brownian motion-driven processes with or without some linear drift terms. To start with, we just input  $\widehat{v_\epsilon^0}(\omega)$ :

$$\begin{aligned}
\widehat{v_\epsilon^0}(\omega) &= \int_{-\infty}^{\infty} e^{i\omega x} [e^{-\epsilon x} v^0(x)] dx \\
&= \int_{-\infty}^{\infty} e^{i\omega x} [e^{-\epsilon x} h(x)] dx.
\end{aligned} \tag{5.62}$$

where  $h(x)$  is the payoff. For call options,  $h(x) = (S_0 e^x - K)_+$ . The factor  $\epsilon$  and the grid width  $w$  should be chosen such that  $e^{w(1-\epsilon)} \rightarrow 0$ , so  $\epsilon > 1$ . For put options,  $h(x) = (K - S_0 e^x)_+$ , then we choose  $\epsilon < 0$  so that  $e^{w\epsilon} \rightarrow 0$ . Then, given  $\widehat{v}_\epsilon^m(\omega)$ , we apply the NFFT to evaluate  $v^m(X)$  at unevenly spaced points  $X(x, t)$  by (5.61) and apply the IFFT to get  $\widehat{v}_{X,\epsilon}^m(\omega)$  by (5.60).  $\widehat{v}_\epsilon^{m+1}(\omega)$  can be obtained by formula (5.59). Finally, we will get  $\widehat{v}_\epsilon^M(\omega)$ , which implies the option price

$$\begin{aligned} P &= e^{-rT} v(x_0, T) = e^{-rT} v^M(x_0) \\ &= e^{-rT} \frac{e^{\epsilon x_0}}{2\pi} \int_{-\infty}^{\infty} \widehat{v}_\epsilon^M(\omega) e^{i\omega x_0} d\omega. \end{aligned} \quad (5.63)$$

The advantage of this algorithm is that we can compute  $v^m(x)$  at each time step  $m$  so that we can compare it with the payoff continuously during the algorithm and take the maximum as the new  $v^m(x)$  to approximate the value of an American option. We just set

$$v^m(x) = \max(v^m(x), e^{rt^m} h(x)) \quad (5.64)$$

at each step to get this approximation.

The algorithm can be summarized in Algorithm 4. The computational complexity is  $\mathcal{O}(4M(N \log N) + MI)$  for American options and  $\mathcal{O}(2(M+1)N \log N + MI)$  for European options, since we do not need  $v^m(x)$  at each step for the European ones.  $I$  denotes the number of unevenly-spaced points.

In our algorithm, we only need to find  $X(x, t)$  with respect to the given drift  $\mu(x)$  to implement the semi-Lagrangian method and input the characteristic function for a given Lévy process  $L_t$ , then the price of European and American options can be calculated.

---

**Algorithm 4** Option pricing through PIDE
 

---

1. Choose a fine grid  $[-w, w]$  with  $N$  points and  $\epsilon$ .
  2. Compute  $v^0(x) = h(x)$ .
  3. Loop  $m = 1$  to  $M$ . **Input:**  $v^m(x)$ .
    - Evaluate  $\widehat{v}_\epsilon^m(\omega)$  by the IFFT.
    - Deduce the unevenly-spaced grid  $X = X(x, t^m)$ .
    - Evaluate  $v^m(X)$  on the unevenly-spaced grid via the NFFT.
    - Evaluate  $\widehat{v}_{X,\epsilon}^m(\omega)$  by the IFFT.
    - Compute  $\widehat{v}_\epsilon^{m+1}(\omega)$  by (5.59).
    - For European option, evaluate  $v^{m+1}(x)$  by taking the FFT.
    - For American option,  $v^{m+1}(x) = \max(v^{m+1}(x), e^{rt^{m+1}}h(x))$ .
 End Loop. **Output:**  $v^{m+1}(x)$ .
  4. Compute option price  $P = e^{-rT}v^M(x_0)$ .
- 

$$\begin{array}{ccc}
 \text{Fourier space:} & \widehat{v}_\epsilon^m(\omega) & \widehat{v}_{X,\epsilon}^m(\omega) \xrightarrow{(5.59)} \widehat{v}_\epsilon^{m+1}(\omega) \\
 & \text{NFFT} \downarrow & \uparrow \text{IFFT} \\
 \text{Real space:} & v^m(X)(\text{uneven}) & \xrightarrow{X=X(x,t^m)} v^m(X(x))(even)
 \end{array}$$

### 5.3.1 Simple Examples

The algorithm is compatible with simple underlying processes, which include the exponential Lévy models discussed in Section 1.2.3 and the Brownian motion-driven OU process in Section 5.2. Such simple examples are presented here to verify our algorithm.

Since we only need  $X(x, t)$  and the characteristic function  $\phi(\omega)$  to implement our algorithm, in terms of exponential Lévy models, we let the drift term  $\mu(x) = r - q + \omega$ , where  $\omega = -\psi(-i)$ . Then  $X(x, t) = x + (r - q + \omega) \cdot (t^{m+1} - t)$ , and  $\phi(\omega)$  is just the characteristic function of  $L_t$ . One could also include the drift term  $r - q + \omega$

in the Lévy process  $L_t$ . Actually, in this case, the NFFT is not necessary to deal with  $X(x, t)$ , and just the FFT is enough to speed up the computation. We need to choose a fine grid  $w$  and  $\epsilon$ . Besides, we consider the convergence rate of our algorithm. For reasons of space, we just show the cases when the number of grid points  $N = 2M$  where  $M$  is the time steps. The result when  $M$  is large enough is used as our reference result. The absolute error is defined as:

$$\text{Error} = |P - P_{ref}/P_{ref}|. \quad (5.65)$$

We consider the American put option under Variance Gamma:  $S_0 = 1369.41$ ,  $K = 1200.0$ ,  $T = 0.56164$ ,  $r = 0.0541$ ,  $q = 0.012$ ,  $\theta = -0.22898$ ,  $\sigma = 0.20722$ ,  $\nu = 0.50215$ . We set grid width  $w = 7$  and  $\epsilon = -3$ . The quoted price is 35.5301 from Hirta and Madan [40]. The reference price of our algorithm is 35.49278528 when  $M = 16000$ .

The European put option under CGMY:  $S_0 = 1$ ,  $K = 1$ ,  $T = 1$ ,  $r = 0.1$ ,  $q = 0$ ,  $C = 1$ ,  $G = 5$ ,  $M = 5$  and  $Y = 0.5$ . We set grid width  $w = 7$  and  $\epsilon = -3$ . The quoted price is 0.10296691 from Almendral and Oosterlee [3]. The reference price of our algorithm is 0.1029669509 when  $M = 16000$ .

Their pricing results are listed in Table 5.3 and 5.4 and Figure 5.1 shows the relative error of these two examples.

As seen in Section 5.2, the price of European call options under Brownian motion-driven OU process has an analytical solution so that it can be used to check our algorithm. We let the Lévy process  $L_t = \sigma W_t$ . Its characteristic function is given by  $\phi(\omega, \Delta t) = -\frac{\sigma^2 \omega^2}{2} \Delta t$ . We also need to find  $X(x, t)$  when  $\mu(x) = a - bx$ . We solve

Table 5.3: Prices of American puts under Variance Gamma

$M$	$N$	Price	Error	CPU time
500	1000	35.48641076	1.796E-4	0.49
1000	2000	35.49071712	5.827E-5	2.18
2000	4000	35.49132480	4.115E-5	9.89
4000	8000	35.49204823	2.077E-5	39.13
8000	16000	35.49260105	5.191E-6	149.19

Table 5.4: Prices of European puts under CGMY

$M$	$N$	Price	Error	CPU time
500	1000	0.1029628114	4.0202E-5	0.0058
1000	2000	0.1029659191	1.0002E-5	0.0075
2000	4000	0.1029666960	2.4757E-6	0.0154
4000	8000	0.1029668902	5.8946E-7	0.0302
8000	16000	0.1029669387	1.1789E-7	0.0734

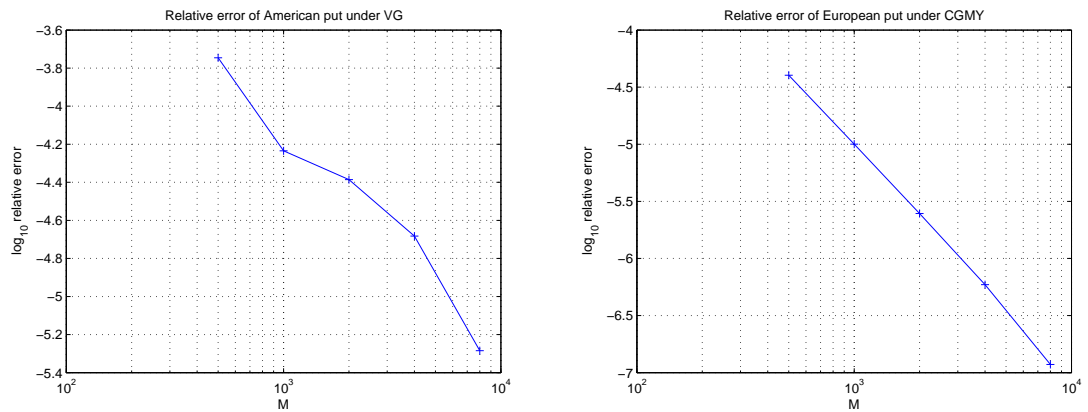


Figure 5.1: Left: Relative error of American puts under Variance Gamma. Right: Relative error of European puts under CGMY.

Table 5.5: Prices of European calls under the OU process

$M$	$N$	Price	Error	CPU time
500	64	24.80703952	1.135E-5	0.73
1000	128	24.80716788	6.178E-6	2.59
2000	256	24.80723695	3.394E-6	9.74
4000	512	24.80728016	1.653E-6	38.04
8000	1024	24.80729963	8.674E-7	176.30

the following ODE

$$\frac{dX}{dt} = bX - a, \quad (5.66)$$

with  $X(x, t^{m+1}) = x$ . We get

$$X(x, t) = xe^{b(t-t^{m+1})} - \frac{a}{b} \left( e^{b(t-t^{m+1})} - 1 \right). \quad (5.67)$$

We still use the same set of parameters as in Section 5.2.1.  $a = 0.2$ ,  $b = 0.5$ ,  $\sigma = 0.1$ ,  $r = 0.1$ ,  $T = 1$ ,  $S_0 = 100$  and  $K = 90$ . We set the grid width  $w = 2.5$ ,  $\epsilon = 8$  and the degree of the NFFT polynomial  $m = 15$ . The exact price of European call in this case is 24.80732115 provided by (5.23). The price of our algorithm is presented in Table 5.5 and the relative error defined as (5.65) is shown in Figure 5.2.

### 5.3.2 Variance Gamma-Driven OU Processes

The advantage of our method is that it enables us to deal with general Lévy processes with non-constant drifts, say the OU mean-reverting drift driven by the Variance Gamma process (OU-VG). In this section, I will present an example of pricing European and American put options in this case.

We assume that in the risk-neutral world, the dynamics of the log return  $x_t$

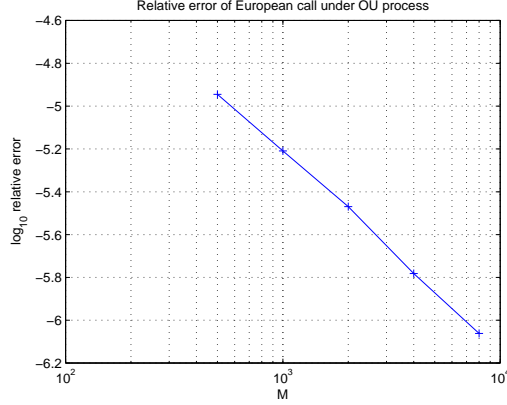


Figure 5.2: Relative error of European calls under the OU process.

follows the following SDE:

$$dx_t = (a - bx_t)dt + dL_t, \quad (5.68)$$

where  $L_t$  is a Variance Gamma process. Of course,  $L_t$  can be any Lévy process, and when  $L_t = \sigma W_t$ , it reduces to the simple OU process discussed in the previous section. The only thing we need to implement our algorithm is the function  $X(x, t)$  corresponding to the OU drift  $\mu(x) = a - bx_t$  and the characteristic function of a Variance Gamma process. From (5.67), we have obtained  $X(x, t)$  of the OU drift, which is:

$$X(x, t) = xe^{b(t-t^{m+1})} - \frac{a}{b} \left( e^{b(t-t^{m+1})} - 1 \right). \quad (5.69)$$

and the characteristic function of a Variance Gamma process with parameter  $(\sigma, \nu, \theta)$  is:

$$\phi(\omega, \Delta t) = \left( \frac{1}{1 - i\theta\nu\omega + (\sigma^2\nu/2)\omega^2} \right)^{\Delta t/\nu}. \quad (5.70)$$

Here we use the same parameters as the American put in the last section from Hirsu and Madan [40] with  $S_0 = 1369.41$ ,  $K = 1200.0$ ,  $T = 0.56164$ ,  $r = 0.0541$ ,

Table 5.6: Prices of European puts under OU-VG

$M$	$N$	Price	Error	CPU time
250	256	30.62785840	1.002E-3	2.07
500	512	30.58442947	4.165E-4	4.99
1000	1024	30.59469280	8.105E-5	19.86
2000	2048	30.59565782	4.951E-5	94.25
4000	4096	30.59630475	2.837E-5	378.57

Table 5.7: Prices of American puts under OU-VG

$M$	$N$	Price	Error	CPU time
250	256	37.05025901	7.035E-3	1.36
500	512	37.11888322	5.196E-3	5.08
1000	1024	37.28919849	6.319E-4	20.28
2000	2048	37.30675911	1.612E-4	83.27
4000	4096	37.31020341	6.894E-5	378.38

$q = 0.012$ ,  $\theta = -0.22898$ ,  $\sigma = 0.20722$ ,  $\nu = 0.50215$ . We set the mean-reverting parameters  $a = 0.2$  and  $b = 0.5$ . The grid width is chosen as  $w = 10$ ,  $\epsilon = -3$  and the degree of the NFFT polynomial is  $m = 15$ . The reference price of the European put is 30.59717272 and that of the American put is 37.31277557 when  $M = 8000$  and  $N = 4096$ .

The prices of European and American puts under this OU-VG case are provided in Table 5.6 and 5.7, and the relative error is shown in Figure 5.3. In Figure 5.4, we compare the price of the European puts and American puts in the left plot, from which we find that the price of an American put is always above the payoff. In the right plot, we compare the price of American puts with different maturities, and it shows that the price increases as the maturity increases.

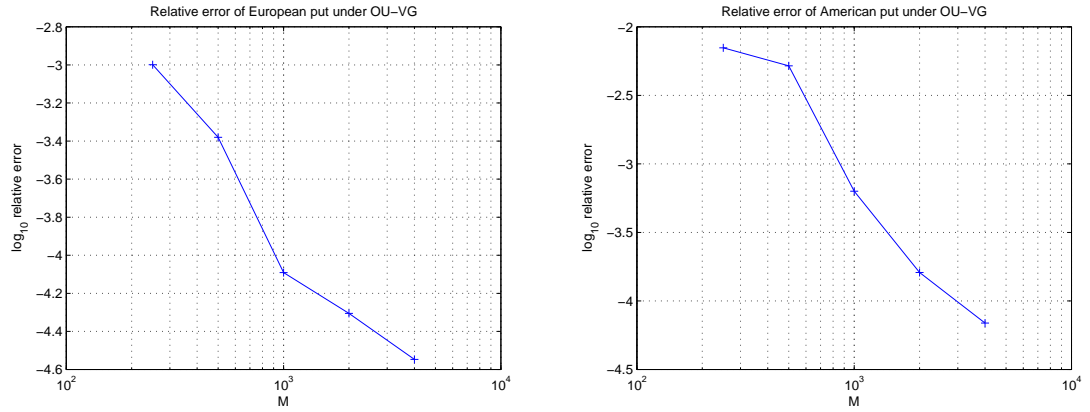


Figure 5.3: Relative error of European puts (left) and American puts (right) under OU-VG.

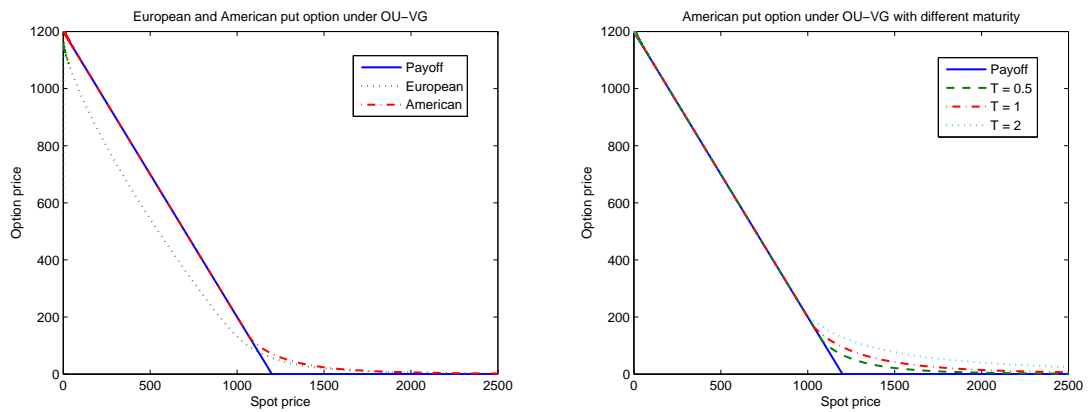


Figure 5.4: Left: Comparison of European and American puts under OU-VG. Right: Comparison of American puts with different maturities under OU-VG.

## Chapter 6

### Conclusion and Future Work

Option contracts are one of the most popular financial derivatives traded in the current markets. The key issue in this area is to determine the values of these contracts, and the first stage is to find an appropriate model that captures the essential behaviour of the underlying markets. Lévy processes are introduced to finance since their underlying distributions are flexible enough to explain some empirical phenomena including negative skewness, high leptokurticity, jumps and volatility smiles. More sophisticated models based on Lévy processes, say mean-reverting models and stochastic volatility models, are also attractive to many researchers. In such Lévy models, Fourier transform techniques have been widely and successfully used in pricing various types of options. This is because the characteristic function is just the Fourier transform of its probability density and there is also a nice relationship between the characteristic exponent and the Fourier transform of the pricing PIDEs associated with the Lévy processes. Therefore, when the characteristic functions are available analytically, the Fourier transform is always ready to help us access the option pricing problems.

This thesis focuses on applying the nonequispaced fast Fourier transform (NFFT) to price various types of options under various underlying processes. The NFFT is a fast approximation to implement the Fourier transform on an unequally spaced grid with computation complexity  $\mathcal{O}(N \log N + M)$ . To start with, we investigated the prices of discrete arithmetic Asian options under the exponential Lévy models. We

applied the NFFT in place of the interpolation in [10] to compute the evolution of the density functions. Compared with the 4th order accuracy of the cubic interpolation method, we demonstrated that the NFFT algorithm offered exponential accuracy by means of highly accurate Gaussian quadrature or Romberg integration. This implies that we can use fewer points to achieve the desired accuracy compared with those in [10, 18]. Because of the fast convergence of the NFFT approach, it is possible for us to approximate the continuous case by increasing the number of observation dates. We matched our results with others both in the discrete approximations and in the semi-analytical continuous solutions. The comparison among different Lévy models for Asian options was also shown.

In addition, we addressed the problem of pricing European and American options via the NFFT when the underlying processes contain some kinds of drift terms. This is based on the semi-Lagrangian method which provides a way to eliminate these drift terms and allows us to deal with some mean-reverting processes. There are two possibilities for doing that: pricing through transition densities and pricing directly. We first considered the pricing problem through the transition densities which are described by a Kolmogorov forward equation. We demonstrated that this method enabled us to price European options under mean-reverting processes driven by a Brownian motion. Our results were verified by analytical solutions in the OU case and by Monte Carlo simulation in the CIR case. Then we moved to price options directly through PIDEs which allowed us to address European and American options under general Lévy-driven processes with non-constant drift terms. In this case, the exponential Lévy models and the Brownian motion driven OU processes are just special examples of our model. We reproduced similar results of other authors'

methods for various types of options and underlying processes. Finally, we proposed an example of pricing European and American put options under Variance Gamma-driven OU processes to show the advantage of our algorithm. We demonstrated the convergence of our method and showed the difference between the prices of European options and American options.

In future research, lots of directions can be considered to extend the applications of the NFFT method in option pricing. We can investigate the possibility to price other path dependent options, for example, barrier options and lookback options. As long as we formulate the recursive form of the evolution of the density functions which is nonlinear, we can always apply the NFFT to replace the interpolation to obtain high order of accuracy. We can also consider American type of Asian options or Asian options on multi-asset. Besides, follow the idea of [44], we can apply the NFFT method based on the semi-Lagrangian scheme to price other exotic options when the underlying processes is driven by Lévy processes with mean-reverting drifts. These options may include barrier options, shout options, spread options and catastrophe options in multi-asset cases or we may also incorporate regime-switching into our model. Here we may need the multi-variate NFFT to implement multi-asset cases and fortunately, it is available in [46]. Furthermore, we could also consider other mean-reverting drifts like the CIR process or Pilipović mean-reverting model. This may require some kind of transform at the beginning to simplify these processes.

# Appendix A

## Background

### A.1 Statistics of Random Variables

For a given random variable  $x$ , we use mean, variance, skewness and kurtosis to characterize the probability distribution of  $x$ . They are defined as follows and are used to describe various distributions throughout this thesis.

- Mean:  $Mean(x) = \mathbb{E}[x]$ ,
- Variance:  $Var(x) = \mathbb{E}[(x - \mu)^2]$ ,
- Skewness:  $Skew(x) = \frac{\mathbb{E}[(x-\mu)^3]}{\sigma^3}$ ,
- Kurtosis:  $Kurt(x) = \frac{\mathbb{E}[(x-\mu)^4]}{\sigma^4}$ ,

where  $\mu = \mathbb{E}[x]$ , and  $\sigma^2 = Var(x)$ .

Skewness measures the asymmetry of a distribution. The normal distribution has zero skewness. A negative skewness distribution has a longer left tail than the right, or say the mass of such a distribution is concentrated on the right part. The kurtosis measures the peakedness of a distribution. The kurtosis of the normal distribution is 3. A distribution with kurtosis greater than 3 is leptokurtic, which means the distribution has higher peak or fatter tails than the normal distribution.

## A.2 Risk-neutral Pricing Theory

Some basic but important concepts in stochastic calculus and mathematical finance are introduced here. Most of these definitions, properties and formulae can be found in [22, 63]

### Martingales

**Definition A.2.1** (Martingale). Given a probability space  $(\Omega, \mathcal{F}, \mathbb{P})$  with a filtration  $\mathcal{F}_t$ , a cadlag process  $(M_t)_{t \in [0, T]}$  is a martingale if  $M$  is adapted to  $\mathcal{F}_t$ ,  $\mathbb{E}[|M_t|]$  is finite for  $t \in [0, T]$  and

$$\mathbb{E}[M_s | \mathcal{F}_t] = M_t, \quad \forall s > t. \quad (\text{A.1})$$

This is a crucial concept to establish the non-arbitrage pricing theory in mathematical finance. For Lévy processes, different martingales can be constructed from their independent increments property.

**Proposition A.2.2.** *Let  $(X_t)_{t \geq 0}$  be a real-valued process with independent increments. Then*

- $\left( \frac{e^{iuX_t}}{\mathbb{E}[e^{iuX_t}]} \right)$  is a martingale,  $\forall u \in \mathbb{R}$ .
- If for some  $u \in \mathbb{R}$ ,  $\mathbb{E}[e^{uX_t}] < \infty$ ,  $\forall t > 0$ , then  $\left( \frac{e^{uX_t}}{\mathbb{E}[e^{uX_t}]} \right)$  is a martingale.
- If  $\mathbb{E}[X_t] < 0$ ,  $\forall t \geq 0$ , then  $M_t = X_t - \mathbb{E}[X_t]$  is a martingale.
- If  $\text{Var}[X_t] < \infty$ ,  $\forall t \geq 0$ , then  $(M_t)^2 - \mathbb{E}[(M_t)^2]$  is a martingale, where  $M$  is the martingale defined above.

### Itô Formula

**Definition A.2.3** (Itô process). Let  $W_t$  be a Brownian motion and  $\mathcal{F}_t$  an associated filtration. An Itô process is defined as

$$X_t = X_0 + \int_0^t \mu(u)du + \int_0^t \sigma(u)dW_u, \quad (\text{A.2})$$

where  $\mu(u), \sigma(u)$  is adapted stochastic processes.

**Theorem A.2.4** (Itô formula for Itô processes). Let  $(X_t)_{t \geq 0}$  be an Itô process and  $f(t, x)$  be a twice differentiable function. Then

$$f(t, X_t) = f(0, X_0) + \int_0^t f_s(s, X_s)ds + \int_0^t f_x(s, X_s)dX_s + \frac{1}{2} \int_0^t f_{xx}(s, X_s)d[X_s, X_s]. \quad (\text{A.3})$$

**Theorem A.2.5** (Itô formula for Lévy processes). Let  $(X_t)_{t \geq 0}$  be a Lévy process with triplet  $(\gamma, \sigma^2, \nu)$  and  $f(t, x)$  be a twice differentiable function. Then

$$\begin{aligned} f(t, X_t) &= f(0, X_0) + \int_0^t [f_s(s, X_s) + \frac{\sigma^2}{2} f_{xx}(s, X_s)]ds + \int_0^t f_x(s, X_{s-})dX_s \\ &\quad + \sum_{0 \leq s \leq t} [f(s, X_{s-} + \Delta X_s) - f(s, X_s) - \Delta X_s f_x(s, X_{s-})]. \end{aligned} \quad (\text{A.4})$$

### Equivalent Martingale Measure

**Definition A.2.6** (Equivalent Martingale Measure). A probability measure  $\mathbb{Q}$  on the probability space  $(\Omega, \mathcal{F}, \mathbb{P})$  is an equivalent martingale measure of  $\mathbb{P}$  if

- $\mathbb{Q}$  is equivalent to  $\mathbb{P}$ , i.e. they have the same null sets.
- The discounted stock price  $\tilde{S}_t = e^{-rt}S_t$  is a martingale under  $\mathbb{Q}$ .

The existence of an equivalent martingale measure (EMM) implies the absence of arbitrage, while the uniqueness of the EMM implies market completeness. If there exists an EMM, we say that we are in the risk-neutral world and non-arbitrage pricing theory can be applied to evaluate financial derivatives. However, the EMM is always not unique, for example, if we are in the exponential Lévy models or mean-reverting world. Several techniques dealing with finding an EMM, say Esscher transform [35] or mean correcting, have been developed.

### Risk-neutral Pricing Formula

If we are in the risk-neutral measure  $\mathbb{Q}$ , then the discounted stock price  $e^{-rt}S_t$  is a martingale. The dynamics of the value of portfolio  $\Pi_t$  can be written as

$$d\Pi_t = \Delta_t dS_t + r(\Pi_t - \Delta_t S_t)dt, \quad (\text{A.5})$$

where  $\Delta_t$  is the share of stock in the portfolio at  $t$ . If we apply the Itô formula to the discounted value of portfolio  $e^{-rt}\Pi_t$ , it turns out to be a martingale under this risk-neutral measure  $\mathbb{Q}$ . By arbitrage free argument, the value of portfolio  $\Pi_t = V_t$  for all  $t \in [0, T]$ , where  $V_t$  is the value of a option. And by the definition of a martingale, we have

$$e^{-rt}V_t = \mathbb{E}^{\mathbb{Q}}[e^{-rT}V_T | \mathcal{F}_t]. \quad (\text{A.6})$$

Let  $f(S, T, K)$  be the payoff function, we have  $V_T = f(S, T, K)$  and rearrangement of (A.6) leads to the risk-neutral pricing formula

$$V_t = \mathbb{E}^{\mathbb{Q}}[e^{-r(T-t)}f(S, T, K) | \mathcal{F}_t]. \quad (\text{A.7})$$

### A.3 Gaussian Quadrature and Romberg Integration

The trapezoid rule and Simpson's rule are two fundamental numerical methods to compute a integral  $\int_a^b f(x)dx$ . If  $[a, b]$  is divided into  $n$  equal subintervals, the orders of error of them are  $\mathcal{O}(h^2)$  and  $\mathcal{O}(h^4)$  respectively, where  $h = (b - a)/n$ . As for the highly accurate numerical integrations, two widely used techniques are Gaussian quadrature and Romberg integration, which are briefly introduced in this section (see [48, 56] for details).

#### Gaussian Quadrature

Generally speaking, the Gaussian quadrature compute the following form of integration by approximation:

$$\int_a^b \omega(x)f(x)dx \approx \sum_{i=1}^n w_i f(x_i). \quad (\text{A.8})$$

The grid points  $x_i$  are no longer equally spaced and weights  $w_i$  are chosen craftily. If  $\omega(x) = 1$  and  $[a, b] = [-1, 1]$ , it is called Gauss-Legendre quadrature. We could find the  $n$  grid points and weights by the default algorithm [39]. First, the grid points  $x_i$  are the roots of the Legendre polynomial  $P_n$ . After this, the weight  $w_i$  is given by:

$$w_i = \frac{2}{(1 - x_i^2)(P'_n(x_i))^2}. \quad (\text{A.9})$$

Then the integration can be compute by

$$\int_a^b f(x)dx = \frac{b-a}{2} \int_{-1}^1 f(u)du, \quad (\text{A.10})$$

where

$$x = \frac{b+a}{2} + \frac{b-a}{2}u.$$

The error of this Gaussian-Legendre quadrature is  $\mathcal{O}\left(\frac{2^{2n+1}(n!)^4}{(2n+1)[(2n)!]^3}\right)$ .

## Romberg Integration

Romberg's method [59] compute the following integral at equally spaced points:

$$\int_a^b f(x)dx, \quad (\text{A.11})$$

by using Richardson extrapolation repeatedly on the trapezoid rule. It can be viewed as the generalization of the Simpson's rule.

If  $f(x)$  is on a grid with  $2^N$  points, the method can be defined inductively by:

$$R_0^0 = \frac{1}{2}(b-a)(f(a) + f(b)) \quad (\text{A.12})$$

$$R_n^0 = \frac{1}{2}R_{n-1}^0 + h_n \sum_{k=1}^{2^{n-1}} f(a + (2k-1)h_n) \quad (\text{A.13})$$

$$R_n^m = \frac{1}{4^m - 1}(4^m R_n^{m-1} - R_{n-1}^{m-1}) \quad (\text{A.14})$$

where  $h_n = \frac{b-a}{2^n}$ , and  $n, m = 1 \dots N$ .

It will produce the following table to illustrate:

$n$	$R_n^0$	$R_n^1$	$R_n^2$	$\dots$	$R_n^N$
0	$R_0^0$				
1	$R_1^0$	$R_1^1$			
2	$R_2^0$	$R_2^1$	$R_2^2$		
$\vdots$	$\vdots$	$\vdots$	$\vdots$	$\ddots$	
$N$	$R_N^0$	$R_N^1$	$R_N^2$	$\dots$	$R_N^N$

The first column  $R_n^0$  is the compound trapezoid rule and the second column  $R_n^1$  is the compound Simpson's rule. The answer  $R_N^N$  is the Romberg approximation with error  $\mathcal{O}(h_N^{2(N+1)})$ .

# Appendix B

## Special Functions and Processes

### B.1 Special Functions

#### Gamma Function

The Gamma function is an extension of the factorial function to real and complex numbers. For a complex number  $z$  with positive real part  $\Re(z) > 0$ , it is defined by

$$\Gamma(z) = \int_0^{\infty} t^{z-1} e^{-t} dt. \quad (\text{B.1})$$

Using integration by parts, one can show that  $\Gamma(z+1) = z\Gamma(z)$ , and one could also get that  $\Gamma(1) = 1$ . These two relations lead to

$$\Gamma(n) = (n-1)!, \quad \forall n \in \mathbb{N}, \quad (\text{B.2})$$

which shows that the factorial function is just a special case of the Gamma function.

#### Bessel Functions

Bessel functions are first defined by Daniel Bernoulli and generalized by Friedrich Bessel. They are solutions to Bessel's differential equation:

$$z^2 \frac{d^2 w}{dz^2} + z \frac{dw}{dz} + (z^2 - \nu^2)w = 0. \quad (\text{B.3})$$

Since this is a second-order differential equation, there must be two linearly independent solutions. Depending upon the circumstances, however, various formulations of

these solutions are convenient, and the different variations are described below:

Bessel functions of the first kind  $J_\nu$ :

$$J_\nu(z) = \left(\frac{z}{2}\right)^\nu \sum_{k=0}^{\infty} \frac{(-z^2/4)^k}{k! \Gamma(\nu + k + 1)}, \quad (\text{B.4})$$

where  $\Gamma(z)$  is the Gamma function.

Bessel functions of the second kind  $Y_\nu$ :

$$Y_\nu(z) = \frac{J_\nu(z) \cos(\nu\pi) - J_{-\nu}(z)}{\sin(\nu\pi)}, \quad (\text{B.5})$$

and for an integer  $n$ ,  $Y_n$  is interpreted in the limiting sense:

$$Y_n(z) = \lim_{\nu \rightarrow n} Y_\nu(z).$$

Bessel functions of the third kind  $H_\nu^{(1)}$  and  $H_\nu^{(2)}$ :

$$\begin{aligned} H_\nu^{(1)}(z) &= J_\nu(z) + iY_\nu(z), \\ H_\nu^{(2)}(z) &= J_\nu(z) - iY_\nu(z). \end{aligned} \quad (\text{B.6})$$

Some useful properties are listed below. For integer order  $n$ ,

$$J_{-n}(z) = (-1)^n J_n(z),$$

$$Y_{-n}(z) = (-1)^n Y_n(z),$$

and for all order  $\nu$ ,

$$H_{-\nu}^{(1)}(z) = e^{i\pi\nu} H_\nu^{(1)}(z),$$

$$H_{-\nu}^{(2)}(z) = e^{-i\pi\nu} H_\nu^{(2)}(z).$$

## Modified Bessel Functions

Modified Bessel functions are also called Bessel functions of imaginary argument.

They are actually the solutions to the following differential equation:

$$z^2 \frac{d^2 w}{dz^2} + z \frac{dw}{dz} - (z^2 + \nu^2)w = 0. \quad (\text{B.7})$$

Modified Bessel functions of the first kind  $I_\nu$ :

$$I_\nu(z) = \left(\frac{z}{2}\right)^\nu \sum_{k=0}^{\infty} \frac{(z^2/4)^k}{k! \Gamma(\nu + k + 1)}, \quad (\text{B.8})$$

where  $\Gamma(z)$  is the Gamma function.

Modified Bessel functions of the second kind  $K_\nu$ :

$$K_\nu(z) = \frac{\pi}{2} \frac{I_{-\nu}(z) - I_\nu(z)}{\sin(\nu\pi)}, \quad (\text{B.9})$$

and for an integer  $n$ ,  $K_n$  is interpreted in the limiting sense:

$$K_n(z) = \lim_{\nu \rightarrow n} K_\nu(z).$$

Some useful properties are listed below. For integer order  $n$ ,

$$I_{-n}(z) = I_n(z),$$

and for all order  $\nu$ ,

$$K_{-\nu}(z) = K_\nu(z).$$

Relation with Bessel functions is given by:

$$I_\nu(z) = e^{-i\pi\nu/2} J_\nu(iz),$$

$$K_\nu(z) = \frac{\pi}{2} e^{i\pi(\nu+1)/2} H_\nu^{(1)}(iz).$$

## B.2 Basic Lévy Processes

### Gamma Process

The gamma process  $X_G(t; \mu, \nu)$  with parameters  $\mu, \nu > 0$  is a stochastic process which starts at zero and has stationary and independent gamma-distributed increments.

The probability density function of a gamma process is given by

$$f_G(x, t) = \left(\frac{\mu}{\nu}\right)^{\frac{\mu^2}{\nu}t} \frac{x^{\frac{\mu^2}{\nu}t-1} e^{-\frac{\mu}{\nu}x}}{\Gamma\left(\frac{\mu^2}{\nu}t\right)}, \quad x > 0, \quad (\text{B.10})$$

where  $\Gamma(z)$  is the gamma function. The characteristic function is given by

$$\phi_G(u, t) = \left(1 - \frac{i u \nu}{\mu}\right)^{-\frac{\mu^2}{\nu}t}. \quad (\text{B.11})$$

The Lévy triplet  $(\gamma, \sigma^2, \nu)$  of the gamma process is given by

$$\left(\mu(1 - e^{\frac{\mu}{\nu}}), 0, \frac{\mu^2}{\nu} \frac{e^{-\frac{\mu}{\nu}x}}{x} 1_{\{x>0\}}\right).$$

The standard moments of the gamma process are as follows:

Standard moments of Gamma process	
Mean	$\mu t$
Variance	$\nu t$
Skewness	$2\sqrt{\nu}/\mu\sqrt{t}$
Kurtosis	$3(1 + 2\nu/\mu^2 t)$

### Inverse Gaussian Process

The inverse Gaussian process  $X_{IG}(t; \delta, \gamma)$  with parameters  $\delta, \gamma > 0$  is a stochastic process which starts at zero and has stationary and independent inverse Gaussian-

distributed increments. The probability density function of a inverse Gaussian process is given by

$$f_{\text{IG}}(x, t) = \frac{\delta t}{\sqrt{2\pi}} x^{-3/2} e^{\delta\gamma t} e^{-(\delta^2 t^2 x^{-1} + \gamma^2 x)/2}, \quad x > 0. \quad (\text{B.12})$$

The characteristic function is given by

$$\phi_{\text{IG}}(u, t) = e^{-\delta t(\sqrt{-2iu + \gamma^2} - \gamma)}. \quad (\text{B.13})$$

The Lévy triplet  $(\alpha, \sigma^2, \nu)$  of the inverse Gaussian process is given by

$$\begin{aligned} \sigma^2 &= 0, \\ \nu_{\text{IG}}(x) &= \frac{\delta}{\sqrt{2\pi}} x^{-3/2} e^{-\gamma^2 x/2} \mathbf{1}_{\{x>0\}}, \\ \alpha &= \frac{\delta}{\gamma} (2N(\gamma) - 1), \end{aligned}$$

where  $N(x)$  stands for the cumulative distribution function of the normal distribution. The standard moments of the inverse Gaussian process are as follows:

Standard moments of inverse Gaussian process	
Mean	$\delta t/\gamma$
Variance	$\delta t/\gamma^3$
Skewness	$3/\sqrt{\delta\gamma t}$
Kurtosis	$3(1 + 5/\delta\gamma t)$

## Bibliography

- [1] A. Almendral, *Numerical valuation of American options under the CGMY process*, in Exotic Option Pricing and Advanced Lévy Models (Chichester, UK), Wiley, 2005.
- [2] A. Almendral and C. W. Oosterlee, *Numerical valuation of options with jumps in the underlying*, Applied Numerical Mathematics **53** (2005), 1–18.
- [3] A. Almendral and C. W. Oosterlee, *Accurate evaluation of European and American options under the CGMY process*, SIAM Journal on Scientific Computing **29** (2007), no. 1, 93–117.
- [4] A. Almendral and C. W. Oosterlee, *On American Options under the Variance Gamma process*, Applied Mathematical Finance **14** (2007), no. 2, 131–152.
- [5] C. Anderson and M. D. Dahleh, *Rapid computation of the discrete Fourier transform*, SIAM Journal of Scientific Computing **17** (1996), 913–919.
- [6] D. Applebaum, *Lévy processes and stochastic calculus*, 1st ed., Cambridge Studies in Advanced Mathematics, Cambridge University Press, July 2004.
- [7] O. E. Barndorff-Nielsen, *Normal inverse gaussian distributions and stochastic volatility modelling*, Scandinavian Journal of Statistics **24** (1997), 1–13.
- [8] O. E. Barndorff-Nielsen, *Processes of normal inverse gaussian type*, Finance and Stochastics **2** (1998), 41–68.

- [9] D. S. Bates, *Jumps and stochastic volatility: Exchange rate processes implicit in deutsche mark options*, Review of Financial Studies **9** (1996), no. 1, 69–107.
- [10] E. Benhamou, *Fast Fourier transform for discrete Asian options*, Journal of Computational Finance **6** (2002), no. 1, 49–68.
- [11] J. P. Benque, G. Labadie, and J. Ronat, *A new finite element method for navier-stokes equations coupled with a temperature equation*, 4th Int. Symp. on Finite Elements Methods in Flow Problems (North Holland) (T. Kawai, ed.), 1982, pp. 295–301.
- [12] F. Black and M. Scholes, *The pricing of options and corporate liabilities*, The Journal of Political Economy **81** (1973), no. 3, 637–654.
- [13] L. Bonaventura, *An introduction to semi - Lagrangian methods for geophysical scale flows*, Lecture Notes, ERCOFTAC Leonhard Euler Lectures, SAM-ETH Zurich, 2004.
- [14] P. Boyle, *Options: a Monte Carlo approach*, Journal of Financial Economics **4** (1977), 323–338.
- [15] P. Carr, H. Geman, D. Madan, and M. Yor, *Stochastic volatility for Lévy processes*, Mathematical Finance **13** (2003), no. 3, 345–382.
- [16] P. Carr, H. Geman, D. B. Madan, and M. Yor, *The fine structure of asset returns: An empirical investigation*, The Journal of Business **75** (2002), no. 2, 305–332.

- [17] P. Carr and D. B. Madan, *Option valuation using the Fast Fourier Transform*, Journal of Computational Finance **2** (1999), 61–73.
- [18] A. Carverhill and L. Clewlow, *Flexible convolution*, Risk **3** (1990), 25–29.
- [19] K.-W. Chen and Y.-D. Lyuu, *Accurate pricing formulas for Asian options*, Applied Mathematics and Computation **188** (2007), no. 2, 1711–1724.
- [20] C. Chiarella and A. Ziogas, *A Fourier Transform analysis of the american call option on assets driven by jump-diffusion processes*, Research paper, University of Technology Sydney, May 2006.
- [21] R. Cont, *Empirical properties of asset returns: stylized facts and statistical issues*, Quantitative Finance **1** (2001), 223–236.
- [22] R. Cont and P. Tankov, *Financial modelling with jump processes*, 1st ed., Financial Mathematics Series, Chapman & Hall / CRC Press, December 2003.
- [23] R. Courant, E. Isaacson, and M. Rees, *On the solution of nonlinear hyperbolic differential equations by finite differences*, Communication on Pure and Applied Mathematics **5** (1952), 243–255.
- [24] J. C. Cox, S. A. Ross, and M. Rubinstein, *Option pricing: A simplified approach*, Journal of Financial Economics **7** (1979), 229–263.
- [25] M. Dempster and S. Hong, *Spread option valuation and the Fast Fourier transform*, Research papers in management studies WP 26/2000, The Judge Institute of Management, 2000.

- [26] Y. d'Halluin, P. Forsyth, and K. Vetzal, *Robust numerical methods for contingent claims under jump diffusion processes*, Submitted, August 2003.
- [27] A. Dutt and V. Rokhlin, *Fast Fourier transforms for nonequispaced data, II*, Applied and Computation Harmonic Analysis **2** (1995), 85–100.
- [28] E. Eberlein and K. Prause, *The generalized hyperbolic model: financial derivatives and risk measures*, Fdm preprint 56, University of Freiburg, 1998.
- [29] P. Forsyth, K. Vetzal, and R. Zvan, *Robust numerical methods for PDE models of Asian options*, The Journal of Computational Finance **1** (1998), no. 2, 39–78.
- [30] P. A. Forsyth, K. Vetzal, and R. Zvan, *Convergence of numerical methods for valuing path-dependent options using interpolation*, Review of Derivatives Research **5** (2002), no. 3, 273–314.
- [31] P. A. Forsyth, J. W. Wan, and I. R. Wang, *Robust numerical valuation of European and American options under the CGMY process*, March 2007.
- [32] G. Fusai, *Pricing Asian option via Fourier and Laplace transforms*, Journal of Computational Finance **7** (2004), 87–106.
- [33] C. W. Gardiner, *Handbook of stochastic methods: for physics, chemistry and the natural sciences*, Springer, 2004.
- [34] H. Geman and M. Yor, *Bessel processes, Asian option, and perpetuities*, Mathematical Finance **3** (1993), no. 4, 349–375.
- [35] H. U. Gerber and E. S. W. Shiu, *Option pricing by Esscher-transforms*, Transactions of the Society of Actuaries **46** (1994), 99–191.

- [36] F. X. Giraldo, *Strong and weak lagrange-galerkin spectral element methods for the shallow water equations*, Computers and Mathematics with Applications **45** (2003), 97–121.
- [37] J. M. Harrison and S. R. Pliska, *Martingales and stochastic integrals in the theory of continuous trading*, Stochastic Processes and their Applications **11** (1981), 215–260.
- [38] S. L. Heston, *A closed-form solution for options with stochastic volatility with applications to bond and currency options*, The Review of Financial Studies **6** (1993), no. 2, 327–343.
- [39] F. B. Hildebrand, *Introduction to numerical analysis*, New York: McGraw-Hill, 1956.
- [40] A. Hirta and D. B. Madan, *Pricing American options under Variance Gamma*, Journal of Computational Finance **7** (2004), 63–80.
- [41] W.-Y. Hsu and Y.-D. Lyuu, *A convergent quadratic-time lattice algorithm for pricing European-style Asian options*, Applied Mathematics and Computation **189** (2007), 1099–1123.
- [42] J. Hull and A. White, *Efficient procedures for valuing European and American path-dependent options*, Journal of Derivatives **1** (1993), 21–23.
- [43] K. ito Sato, *Lévy processes and infinitely divisible distributions*, 1st ed., Cambridge Studies in Advanced Mathematics, Cambridge University Press, November 1999.

- [44] K. R. Jackson, S. Jaimungal, and V. Surkov, *Fourier space time-stepping for option pricing with Lévy models*, March 2007.
- [45] K. R. Jackson, S. Jaimungal, and V. Surkov, *Option pricing with regime switching Lévy process using fourier space time stepping*, The 4th IASTED International Conference on Financial Engineering and Applications (P. Locke, ed.), ACTA Press, September 24–26 2007.
- [46] J. Keiner, S. Kunis, and D. Potts, *NFFT 3.0 - Tutorial*, Chemnitz University of Technology, Department of Mathematics, Chemnitz, Germany.
- [47] A. G. Z. Kemna and A. C. F. Vorst, *A pricing method for options based on average asset values*, *Journal of Banking & Finance* **14** (1990), no. 1, 113–129.
- [48] D. R. Kincaid and E. W. Cheney, *Numerical analysis: Mathematics of scientific computing*, 3 ed., Brooks Cole, 2001.
- [49] B. Lapeyre and E. Temam, *Competitive Monte Carlo methods for the pricing of Asian options*, *Journal of Computational Finance* **5** (2001), no. 1, 39–57.
- [50] D. B. Madan and E. Seneta, *The VG model for share market returns*, *Journal of Business* **63** (1990), 511–524.
- [51] D. B. Madan, P. P. Carr, and E. C. Chang, *The Variance Gamma process and option pricing*, *European Finance Review* **2** (1998), 79–105.
- [52] A. M. Matache, P. A. Nitsche, and C. Schwab, *Wavelet Galerkin pricing of American options on Lévy driven assets*, *Quantitative Finance* **5** (2005), no. 4, 403–424.

- [53] D. Nualart and W. Schoutens, *BSDE's and Feynman-Kac formula for Lévy processes with applications in finance*, June 2001.
- [54] C. W. Oosterlee, R. Lord, F. Fang, and F. Bervoets, *A fast and accurate FFT-based method for pricing early-exercise options under Lévy processes*, SIAM Journal on Scientific Computing **30** (2008), no. 4, 1678–1705.
- [55] D. Potts, G. Steidl, and M. Tasche, *Fast Fourier transforms for nonequispaced data: A tutorial*, ch. 12, pp. 249–274, Modern Sampling Theory: Mathematics and Applications, 2001.
- [56] A. Quarteroni, R. Sacco, and F. Saleri, *Numerical mathematics*, Springer, 2000.
- [57] S. Raible, *Lévy processes in finance: Theory, numerics, and empirical facts*, Ph.D. thesis, Freiburg i. Br., 2000.
- [58] L. Rogers and Z. Shi, *The value of an Asian option*, Journal of Applied Probability **32** (1995), no. 4, 1077–1088.
- [59] W. Romberg, *Vereinfachte numerische integration*, Norske Videnskabers Selskab Forhandlinger (Trondheim) **28** (1955), no. 7, 30–36.
- [60] W. Rudin, *Functional analysis*, McGrawHill, 1991.
- [61] W. Schoutens, *The Meixner process in finance*, Eurandom report 2001-002, EURANDOM, Eindhoven, 2001.
- [62] W. Schoutens, *Lévy processes in finance: Pricing financial derivatives (wiley series in probability and statistics)*, Wiley, May 2003.

- [63] S. E. Shreve, *Stochastic calculus for finance II: Continuous-time models*, 1st ed., Springer Finance, Springer, 2004.
- [64] A. Staniforth and J. Cote, *Semi-lagrangian integration schemes for atmospheric models a review*, Monthly Weather Review **119** (1991), no. 9, 2206–2223.
- [65] G. Steidl, *A note on fast Fourier transforms for nonequispaced grids*, Advances in Computational Mathematics **9** (1998), no. 3-4, 337–352.
- [66] E. Suli and A. F. Ware, *A spectral method of characteristics for first-order hyperbolic equations*, SIAM J. Num. Anal. **28** (1991), no. 2, 423–445.
- [67] G. W. P. Thompson, *Fast narrow bounds on the value of Asian options*, Preprint, Cambridge University, 1998.
- [68] L. N. Trefethen, *Spectral methods in MATLAB*, SIAM: Society for Industrial and Applied Mathematics, February 15 2001.
- [69] J. Vecer, *A new PDE approach for pricing arithmetic average Asian options*, The Journal of Computational Finance **4** (2001), no. 4, 105–113.
- [70] J. Vecer, *Unified Asian pricing*, Risk **15** (2002), no. 6, 113–116.
- [71] A. F. Ware, *A Spectral Lagrange Galerkin method for convection dominated diffusion problems*, Ph.D. thesis, University of Oxford, October 1991.
- [72] A. F. Ware, *Fast approximate Fourier transforms for irregularly spaced data*, SIAM Review **40** (1998), 838–856.

- [73] P. Wilmott, S. Howison, and J. Dewynne, *The mathematics of financial derivatives: A student introduction*, Cambridge University Press, September 1995.
- [74] J. Zhang, *A semi-analytical method for pricing and hedging continuously sampled arithmetic average rate options*, *Journal of Computational Finance* **5** (2001), no. 1, 59–79.